Accepted Manuscript

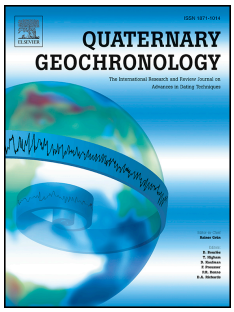

Protein diagenesis in *Patella* shells: implications for amino acid racemisation dating

José E. Ortiz, Igor Gutiérrez-Zugasti, Trinidad Torres, Manuel González-Morales, Yolanda Sánchez-Palencia

PII: S1871-1014(15)00021-7

DOI: 10.1016/j.quageo.2015.02.008

Reference: QUAGEO 634

To appear in: *Quaternary Geochronology*

Received Date: 22 July 2014

Revised Date: 31 January 2015

Accepted Date: 8 February 2015

Please cite this article as: Ortiz, J.E., Gutiérrez-Zugasti, I., Torres, T., González-Morales, M., Sánchez-Palencia, Y., Protein diagenesis in *Patella* shells: implications for amino acid racemisation dating, *Quaternary Geochronology* (2015), doi: 10.1016/j.quageo.2015.02.008.

Protein diagenesis in *Patella* shells: implications for amino acid racemisation dating

José E. Ortiz[a*], Igor Gutiérrez-Zugasti[b], Trinidad Torres[a], Manuel González-Morales[b], Yolanda Sánchez-Palencia[a]

[a]*Laboratory of Biomolecular Stratigraphy, E.T.S.I. Minas, Universidad Politécnica de Madrid. C/ Ríos Rosas 21, Madrid 28003 (Spain)*

[b]*Instituto Internacional de Investigaciones Prehistóricas de Cantabria. Facultad de Filosofía. Universidad de Cantabria. Avda de los Castros s/n 39005 Santander (Spain)*

* corresponding author. Tel. +34 913366970; Email address: joseeugenio.ortiz@upm.es

Abstract

The inter- and intra-crystalline fractions of *Patella vulgata* limpets recovered from archaeological sites in Northern Spain (covering Neolithic, Mesolithic, Magdalenian, Solutrean, and Aurignacian periods) were examined for amino acid composition and racemisation over time. The calcitic apex and rim areas of the shells were found to probably be composed of similar proteins, as the D/L values and amino acids were comparable and varied in the same way with increasing age; however, the mineral structures present in these areas differed. The aragonitic intermediate part of the shell showed a distinctly different

amino acid composition and mineral structure. The main protein leaching from the inter-crystalline fraction occurred within the first 6,000 yr after the death of the organism. In contrast, the intra-crystalline fraction — comprised of a different protein composition than the inter-crystalline fraction — appeared to behave as a closed system for at least 34 ka, as reflected by the lack of a significant decrease in the amino acid content; however, changes in the amino acid percentages occurred during this period. The concentration of aspartic acid remained almost constant with age both in inter- and intra-crystalline proteins, and its contribution to the total amino acid content increased with age at the expense of other amino acids such as glutamic acid, serine, glycine and alanine. Temperature is thought to play a key role in the amino acid racemisation of *P. vulgata* and could explain why in the localities belonging to the Gravettian and Solutrean period, which formed during relatively cold conditions, D/L values were similar to those detected in shells from sites formed during the Magdalenian.

Key-words: *Patella vulgata*, inter- and intra-crystalline proteins, amino acids, microstructure, archaeology

Highlights:

- The calcitic apex and rim of *P. vulgata* shells are probably made of similar proteins
- The aragonitic intermediate area has a different amino acid composition
- The main protein leaching in the inter-crystalline fraction occurs in the first 6 ka

- Asp content remained constant up to 34 ka in inter- and intra-crystalline fractions
- The percentage of aspartic acid increased with age (over ca. 34 ka)

1. Introduction

The first attempts to establish the chronology of shell middens using amino acid racemisation/epimerisation date back to the 1970s when Masters and Bada (1977) and Wehmiller (1977) analysed marine bivalve molluscs (*Chione*) from California. Several studies have demonstrated that amino acid racemisation (AAR) is a satisfactory tool for dating palaeontological and archaeological sites, including the use of limpets recovered from Palaeolithic and Mesolithic anthropogenic shell middens (Bateman, 2008; Ortiz et al., 2009a; Demarchi et al., 2011). Shell middens often accumulate relatively rapidly but they are subject to complex taphonomy. Consequently, large sample sizes for dating are required to resolve issues of intra-site chronology (e.g. Glover et al., 1990; Stein and Deo, 2003).The number of samples commonly used for the age calculation of a single level through AAR allows not only the rejection of anomalous results, but also an understanding of time-averaging and the time over which a certain site formed.

Some uncertainties regarding the protein diagenesis of limpet shells remain. Further research is therefore required to clarify the processes of protein preservation and degradation and the concomitant success of AAR for dating archaeological localities. Recent studies of modern limpets performed by Demarchi et al. (2011, 2013a,b) showed the potential of intra-crystalline proteins in *Patella* shells for AAR geochronology. In these studies, artificial

diagenesis was induced in proteins (both inter- and intra-crystalline protein fractions, and the isolated intra-crystalline fraction) of modern *Patella* shells through high-temperature experiments (80º, 110º, and 140ºC) over a range of times (0 to 5738 h). The protein breakdown was quantified by measuring the extent and racemisation of various amino acids. This provided data on protein diagenesis in modern limpets; however, it is pertinent to reveal the circumstances of protein degradation in fossil representatives. In this regard, here we examined the amino acid content and D/L values in limpets (*Patella vulgata*) collected from several archaeological sites of known ages (dated by ^{14}C) covering the Aurignacian (ca. 34 cal. ka BP), Gravettian (ca. 27.5 cal. ka BP), Solutrean (ca. 26.5-20.5 ka cal. BP), Lower, Middle and Upper Magdalenian (20.5-12.0 cal. ka BP), Azilian (ca. 12.0-10.8 cal. ka BP), Mesolithic-Asturian (10.8-6.3 cal. ka BP), and Neolithic (ca. 6.3-5.8 cal. ka BP) periods. *P. vulgata* was chosen because this limpet is the most common species in shell middens in Northern Spain (González-Morales, 1982; Bailey and Craighead, 2003; Gutiérrez-Zugasti, 2009, 2011; Álvarez-Fernández, 2011). We examined the behaviour of the whole protein content (inter- and intra-crystalline proteins) and the intra-crystalline fraction separately, the latter by bleaching prior to analysis.

Several studies (Haugen and Sejrup, 1992; Wehmiller, 1993; Torres et al., 1999) have reported intra-shell variation of D/L values depending on the part of the carapace from which the sample is recovered. We therefore also studied the amino acid content and D/L values of two parts of the shell (apex and rim) in samples of various ages.

2. Material and methods

The samples were collected from 12 sites in the regions of Asturias and Cantabria (Northern Spain) previously excavated in archaeological campaigns (Fig. 1). Permission was obtained for sampling the limpets. Once collected, the shells were stored at the "Museo Arqueológico de Asturias", the "Museo de Prehistoria y Arqueología de Cantabria", and the "Museo y Centro de Investigación de Altamira". Limpets were cleaned with water after their collection and stored in boxes at room temperature (15ºC) in the museums. The coordinates of the localities are reported in Table 1 (Fig. 1), together with the time period of the archaeological level sampled.

P. vulgata shells from the levels belonging to the Upper Palaeolithic (Aurignacian, Gravettian, Solutrean, Magdalenian, Azilian), Mesolithic (Asturian) and Neolithic (Table 1) periods were analysed for AAR. For comparitive purposes, modern specimens were recovered from Cue beach (Asturias), located close to the archaeological localities (Fig. 1).

2.1 Petrographic analysis

Selected *P. vulgata* shells from modern individuals were cut into thin sections along their major axis and placed on microscope slides. To determine the distribution of minerals and the organic matrix, the sections were submerged in Feigl´s and Mutvei´s solutions for 5 min and observed under a Nikon microscope.

To distinguish between the two calcium carbonate polymorphs that mollusc shells generally form, we applied Feigl´s solution, which was prepared following Feigl (1937, in Friedman 1959). This procedure stained aragonite crystals black, while calcite ones remain unstained.

To highlight the organisation of the organic matrix and the crystal arrangement, we used Mutvei's solution (Mutvei *et al.* 1994), following the modifications described by Schöne *et al.* (2005): one litre of Mutvei's solution consists of 500 ml 1% acetic acid, 500 ml 25% glutaraldehyde and ca. 5 to 10 g Alcian blue powder. The use of Mutvei's solution facilitates the identification of micro-growth structures in carbonates of biogenic origin by staining organic matrix laminae and crystal envelopes in shades of blue.

2.2 Amino acid racemisation

Between 4 and 11 *P. vulgata* shells (analytical samples) from each archaeological level were analysed for amino acids. The use of monospecific or monogeneric samples reduces taxonomically-controlled variability in D/L values (Murray-Wallace, 1995; Murray-Wallace and Goede, 1995). In the laboratory, shells were carefully sonicated and cleaned with water to remove sediment. Peripheral parts, approximately 20–30%, were removed after chemical cleaning of the sample with 2 N HCl.

For all samples, we drilled a small disc in the apex of the shells, which has been shown to reduce variability (cf. Murray-Wallace, 1995). This selection was also based on the results from the petrographic analysis, which showed that the apex was made of calcite (cf. MacClintock, 1967; Fenger et al., 2007, Ortiz et al., 2009a; Demarchi et al., 2013a). In addition, we sampled the rim, also made of calcite, in the same limpets (with the exception of those from La Riera cave) in order t test intra-shell variation. The intermediate part of the shell was also sampled, but only in modern limpets. *ca.* 5–20 mg of apex and rim areas was subjected to AAR analysis of the total protein content (inter- and intra-crystalline proteins).

Samples from the apex were also used to measure the amino acids in the intra-crystalline fraction after bleaching.

2.2.1 Bleaching

Powdered shell samples from the apex of the same limpets used to analyse the total protein content were used for the isolation of intra-crystalline proteins. The shell particles measured less than 500 µm, following Demarchi et al. (2013a), a size for which bleaching is most effective. In this regard, we exposed these powdered samples to 10% sodium hypochlorite (NaOCl), an effective oxidising agent for this purpose (Penkman et al., 2008; Demarchi et al., 2013a). Samples were exposed to NaOCl for 48 h, a time reported to be the optimal bleaching period for *P. vulgata* (Demarchi et al., 2013a), although they used a NaOCl concentration of 12%.

For each fraction, 50 µL of NaOCl per mg of powdered shell was added to accurately weighed subsamples at room temperature. To ensure the complete penetration of the oxidising agent, the vials containing the powders and the bleach were shaken every 24 h. The bleach was then removed, and the powders were rinsed five times in ultrapure water and once in HPLC-grade methanol, with centrifugation or 4 min. between each rinse to minimise the removal of powder. Finally, the samples were air-dried overnight.

2.2.2 Amino acid analysis

Amino acid concentrations and racemisation/epimerisation ratios were quantified using a HPLC, following the sample preparation protocol described in Kaufman and Manley (1998) and Kaufman (2000). This procedure involves hydrolysis, which was performed under an N_2 atmosphere in 20 μL/mg of 7 M HCl for 20 h at 100ºC. The hydrolysates were evaporated to dryness in *vacuo* and then rehydrated in 10 μL/mg of 0.01 M HCl with 1.5 mM sodium azide and 0.03 mM L-*homo*-arginine (internal standard).

Samples were injected into an Agilent HPLC-1100 equipped with a fluorescence detector. Excitation and emission wavelengths were programmed at 335 nm and 445, respectively. A Hypersil BDS C18 reverse-phase column (5 μm; 250 x 4 mm i.d.) was used for the analysis. Derivatisation was achieved before injection by mixing the sample (2 μl) with the pre-column derivatisation reagent (2.2 μl), which comprised 260 mM isobutyryl-L-cysteine (chiral thiol) and 170 mM o-phtaldialdehyde, dissolved in a 1.0 M potassium borate buffer solution at pH 10.4. Eluent A consisted of 23 mM sodium acetate with 1.5 mM sodium azide and 1.3 mM EDTA, adjusted to pH 6.00 with 10 M sodium hydroxide and 10% acetic acid. Eluent B was HPLC-grade methanol, and eluent C consisted of HPLC-grade acetonitrile. A linear gradient was performed at 1.0 mL/min and 25ºC, from 95% eluent A and 5% eluent B upon injection to 76.6% eluent A, 23% eluent B, and 0.4% eluent C at min 31; and then with a progressive gradient at 1.07 mL/min and the following percentages: 46.2% eluent A, 48.8% eluent B, and 5.0% eluent C at min 95. As a laboratory routine, we separated the D and L peaks of the following amino acids (Fig. 1-Supplementary Data): aspartic acid and asparagine (Asx), glutamic acid and glutamine (Glx), serine (Ser), alanine (Ala), valine (Val), phenylalanine (Phe), isoleucine (Ile), leucine (Leu), threonine (Thr), arginine (Arg), and tyrosine (Tyr), together with the abundance of glycine (Gly).

Asx and Glx D/L values obtained by means of HPLC are comparable with those measured with GC as similarities have been reported in inter-laboratory comparison exercises (cf. Wehmiller, 1984; Torres et al., 1997; Wehmiller et al., 2010) and between several samples analyzed by GC and HPLC in our laboratory (cf. Ortiz et al., 2009b, p. 955, see Fig. 2-Supplementary Data).

2.2.3 Data screening of the AAR analyses

A total of 121 powdered samples taken from the apex of *P. vulgata* shells were analysed for amino acid content. The same 121 samples were also used for the bleaching experiment. Rim samples of 76 of these limpets were also used to determine their amino acid composition (samples from the levels of La Riera Cave were not used because we obtained permission to take samples only from the apex).

Of these, 14 results (11.6% of the data- 1 in Kobaederra, 3 in Arenillas, 2 in Mazaculos II, 1 in El Penicial, 1 in Bricia-B, 3 in El Cuco, 2 in level 24 of La Riera, and 1 in level 23 of La Riera 5) were excluded due to Asx and Glx D/L values that fall off the covarience trend (cf. Kaufman, 2003, 2006; Laabs and Kaufman, 2003) (Figs. 3-5 Appendix) and/or because of abnormally high D/L values, characterised by Asx D/L and Glx D/L values falling outside the 2σ range of the group (cf. Hearty et al., 2004; Kosnik and Kaufman, 2008). These samples also showed a low amino acid content. 12.4% of the data from bleached apex samples, and 11.8% from unbleached rim samples were also excluded, coinciding in most cases with outliers from unbleached apex. It is possible that these samples with high D/L values were anthropogenically-heated. Each result and the samples rejected are shown in the

Appendix.The data used in the following sections is only from the screened samples, not including outliers.

2.3 Temperature within the sediment of archaeological sites

As AAR is a temperature-dependent process, we attempted to observe the influence of atmospheric temperature inside the archaeological sites. For this purpose, permission was obtained from the Communities of Asturias and Cantabria to bury Hobo UA-001-64 digital thermometers between 10 and 15 centimetres inside the sediment at the entrance to some of the caves where the remains were collected (El Cuco, Arenillas, El Perro, Mazaculos II, La Riera, Bricia, El Penicial, and La Lloseta). These devices were programmed to register temperature at 4-h intervals and data was collected over 1 year (January to December 2013)..

3. Intrashell variations

3.1 Petrographic analysis

As observed previously (MacClintock, 1967; Fenger et al., 2007; Ortiz et al., 2009a; Demarchi et al. 2013a), calcite was the main component of the apex and rim of modern and archaeological representatives. These shell areas remained unstained after submerging the thin sections in the Feigl dye (Figs. 2A, B), which corresponded to layers M+3, M+2 and M-

224 2 according to the terminology of MacClintock (1967), M being the myostracum (muscle
225 attachment site). In contrast, the intermediate area (layers M+1, M, M-1) was stained black,
226 indicating that it was made of aragonite (Figs. 2A, B). Similar to the findings of MacClintock
227 (1967) and Demarchi et al (2013a), we found that the outer aragonite layer did not occupy a
228 significant portion of the shell.

229 Of note, the boundary between the calcitic M-2 layer and the aragonitic M-1 layer was not
230 straight but showed an interfingering relationship between the two layers (Fig. 2A). This
231 relationship was also observed when the shells were stained with Mutvei's solution (Fig. 2C).
232 This dye revealed major and minor growth lines of biogenic carbonate, both in the calcitic
233 and aragonitic dominions, which were parallel to the shell surface. Major growth lines in the
234 cross-sections were identified as thicker, more pronounced lines, and these were more clearly
235 observed in layers M+1, M-1 and M-2 (Fig. 2C, D). Minor growth lines, representing
236 semidiurnal and lunar growth increments (Fenger et al., 2007), were extremely fine and
237 detected only at high magnification (Fig. 2E).

238 Mutvei's solution also showed an irregular distribution of organic matter through the shell
239 section, as revealed by a strong stain in the calcitic apex (M-2) and rim (M+3, M+2), thus
240 indicating stripes rich in organic matter. In contrast, aragonitic intermediate parts (M+1, M-1)
241 were a brownish colour. In most cases, the outermost M+3 and M+2 layers were not clearly
242 distinguishable, as also reported in Forli et al. (2004).

243 The myostracum was very thin and showed a prismatic structure with large crystals oriented
244 perpendicular to the shell surface (Fig. 2D). In the closest interior and external areas to the
245 myostracum (M-1, M+1 respectively), namely the aragonitic intermediate part, we observed a
246 complex crossed-lamellar structure consisting of complicated hierarchical structural (first-,

247 second- and third-order lamellar structures) features with a feather-like pattern, in which the
248 fibres are oriented perpendicular to the surface of the shell (Fig. 2E, G). Consistent with
249 observations by MacClintock (1967) and Cohen and Branch (1992), we found that the
250 aragonitic M-1 layer was very thin (Fig. 2D, E).

251 In contrast, the microstructure of the rim (M+3, M+2 layers) showed a concentric crossed-
252 lamellar pattern with crystal aggregates arranged parallel to the shell margin, although in
253 these layers (M+2 and M+3) they then became gradually oblique to the outer surface, with a
254 progressive twist to 90º of first order lamella (Fig. 2D, E, F, H), although columnar in
255 appearance. The apex, which was occupied by layer M-2, showed a microstructure with an
256 irregular to radial crossed-lamellar pattern (Fig. 2C).

257 In agreement with Watabe (1984) and Cohen and Branch (1992), the complex crossed-
258 lamellar layers (M-1, M+1) consisted of aragonite, whereas the concentric crossed-lamellar
259 layers (M+3, M+2, M-2) were made of calcite.

260 In brief, layers M+3, M+2 and M-2 were made of calcite and rich in organic matter, although
261 showed different microstructural patterns. In contrast, M+1, M and M-1 layers consisted of
262 aragonite and contain less organic matter. For AAR we analysed the M-2 layer (apex), and
263 M+3 and M+2 layers (rim). In modern representatives we also analysed the M+1 and M-1
264 layers located in the intermediate area.

265

266 ***3.2 Amino acid D/L values***

267

268 ***3.2.1 Apex and rim - unbleached***

The mean Asx and Glx D/L values in the rim and apex of 105 bleached and unbleached *P. vulgata* shells from the archaeological levels (after the rejection of samples with abnormally high D/L values) are shown in Fig. 3. We selected Asx and Glx because they account for a considerable percentage of the amino acid content in modern shells, as shown by Demarchi et al. (2013a).

The individual Asx D/L values in modern limpets were similar in the apex and rim (Fig. 6-Supplementary Data) corresponding with Demarchi et al. (2013a). A similar pattern was obtained for Asx D/L values in these two areas of the shells from the archaeological localities. Similarly, the mean Glx D/L values in the apex and rim of shells from each site were equivalent (Fig. 3, Fig. 7-Supplementary Data, Table 2- Supplementary Data).

In modern limpets we also analysed the amino acids in the intermediate part of the shell, observing that Asx and Glx D/L values were higher than in the apex and rim (Table 2).

3.2.2 Apex - bleached

Asx D/L values were lower in bleached than in unbleached samples for the same individual shell (Fig. 3). In contrast, Glx D/L values were higher in bleached samples than in unbleached ones for modern and archaeological localities.

3.3 Amino acid concentrations

290

291 ***3.3.1 Apex and rim-unbleached***

292

293 The mean of the total amino acid concentration in unbleached *P. vulgata* shells was higher in
294 the rim than in the apex, at least in modern, Neolithic, and Mesolithic limpets (Fig. 4). In
295 contrast, in Palaeolithic limpets the concentration of amino acids in these areas was more
296 similar to each other. Likewise, there was variability in the amount of amino acids present in
297 shells within the same level.

298 Similar results were observed for the individual concentrations of Asx ([Asx]) and Glx
299 ([Glx]) (Fig. 5, 6), two of the most abundant amino acids in limpet shells. Of note, the
300 percentage of each amino acid was similar in the apex and rim areas (Fig. 7).

301 In modern representatives, the total amino acid content, [Asx], and [Glx] were lower in the
302 intermediate parts of shells than in the apex and rim (Table 2). Nevertheless, the percentages
303 of [Asx] and [Glx] in modern specimens were similar to those found in the apex and rim,
304 although the proportion of other amino acids differed (Fig. 8), i.e. %Ser and %Gly were
305 lower in the intermediate part than in the apex and rim areas, while %Ala, %Val and %Leu
306 were higher.

307

308 ***3.3.2 Apex - bleached***

309

The apex intra-crystalline fraction accounted for around 15% of the total proteins within a modern limpet shell (Fig. 4). The amino acid composition of inter- and intra-crystalline proteins in the apex of modern and archaeological limpets also differed, as the percentage of [Asx] was higher in unbleached (40%) than in bleached samples (20–25%) (Table 3), the percentages of [Glx] and [Gly] being higher in the latter. Similar [Asx] percentages were reported by Demarchi et al. (2013a) for bleached and unbleached modern representatives. However, in some other mollusc shells, the percentage of [Asx] has been reported to increase after bleaching (Penkman et al., 2008).

3.4 Interpretation of intrashell variations

3.4.1 Inter-crystalline fraction

Here we observed similar Asx D/L values in the unbleached rim and apex sub-samples of modern limpets and archaeological sites (Fig. 3). This observation is reinforced by the finding that the percentage of each amino acid was similar in the apex and the rim, even with increasing age (Fig. 7). This finding indicates that the proteins comprising these regions are probably similar, both areas being made of calcite (cf. MacClintock, 1967; Fenger et al., 2007, Ortiz et al., 2009a; Demarchi et al., 2013a). It must be highlighted that the acidic amino acids (Asx and Glx) accounted for more than half the content of *Patella* shells. This observation could be associated with the presence of acidic and Asp-rich proteins, which are usually found linked to calcitic structures (Gotliv et al., 2005; Marin et al., 2012). However, we found that the total amino acid content and also the individual concentrations of the two

main amino acids (Asx and Glx) in *P. vulgata* shells were higher in the unbleached rim than in the unbleached apex, at least in modern, Neolithic, and Mesolithic limpets (Fig. 4). These results could be attributable to the different mineral structure observed (Fig. 2). Similarly, differential leaching from the unbleached samples may have produced these differences (cf. Penkman et al., 2007, 2008). Likewise, Demarchi et al. (2013a) reported slightly higher concentrations of amino acids in the unbleached rim of modern representatives when compared with the unbleached bulk samples (rim + apex). Our findings imply that in spite of sampling different parts of the *P. vulgata* shells (apex, rim), there is no significant intra-shell variation of D/L values from the inter-crystalline fraction.

The total concentration of amino acids present in *P. vulgata* shells was variable within the same archaeological level. This observation has also been made in other molluscs (Penkman et al., 2008; Torres et al., 2013) and can be attributed to diverse factors related to the depositional environment, including taphonomical processes such as chemical dissolution, mechanical fragmentation, and bioerosion (Davies et al., 1989; Meldahl et al., 1997; Kidwell, 1998; Carroll et al., 2003; Kidwell et al., 2005), all of which can directly influence the skeletal preservation of shells. Nevertheless, a considerable part of the organic matrix was conserved, thereby reinforcing the notion proposed by Wehmiller (1990) that approximately 30-60% of the original amino acid concentration remains in carbonate Quaternary fossils.

Asx and Glx D/L values in the aragonitic intermediate part of the modern limpet shells (comprising mostly M-1, M, and M+1 layers) were higher than in the apex and rim (Table 2), which are made of calcite (Fig. 2). Also, the percentages of each amino acid differed slightly, as %[Ser] and %[Gly] were lower, whereas %[Ala], %[Val] and %[Leu] were higher than in the apex and rim, thus indicating that other proteins were present, or were represented in differing proportions. These differences were confirmed by the different stain produced in

these layers after submerging the shell cross-sections in Mutvei´s dye, showing that the calcitic M-2, M+2 and M+3 layers were richer in organic matter than the aragonitic M-1 and M+1 layers. According to Marie et al. (2013), Asp-rich proteins, which are more abundant in calcium structures (Sarashina and Endo, 2001; Marin and Luquet, 2004; Gotliv et al., 2005; Marie et al., 2013) are strongly stained with Alcian blue, while other proteins do not show such colouration.

Although differences in the amino acid composition (abundance and percentages) were observed between the aragonitic intermediate part (M+1, M, M-1) and the calcitic apex (M-2) and rim areas (M+2, M+3), there was a high content of acidic amino acids (predominantly Asx) in the whole shell (Fig. 8).

3.4.2 Intra-crystalline fraction

The intra-crystalline proteins represented a small fraction with respect to the total proteins in modern *Patella* shells (ca. 15%) (Fig. 4) in agreement with Demarchi et al. (2013a), who observed that they represented 10% in modern shells. Similar to that observed in the inter-crystalline matrix, acidic amino acids were also abundant in the intra-crystalline fraction, representing 30–35%, vs 45-50% in the inter-crystalline fraction (Table 3). This observation indicates that the inter- and intra-crystalline protein compositions differ, at least in the apex area, thus potentially affecting the AAR rates (Fig. 3). Asx and Glx D/L values were indeed higher in the intra-crystalline fraction of modern limpets.

4. Protein degradation with age

4.1 Amino acid concentrations vs. age

4.1.1 Apex and rim - unbleached

The total amino acid concentration in the apex and rim of unbleached limpet shells (representing the amino acids that comprise inter- and intra-crystalline proteins) was higher in modern specimens than in archaeological ones (Fig. 4); the total amino acid content in the apex decreased by around 40% from modern to Mesolithic limpets. However, the concentrations were similar in archaeological limpets of diverse ages, even in the oldest samples analysed in this study, with the exception of Les Pedroses cave, in which slightly lower concentrations were detected. Limpets from Kobaederra (Neolithic) showed a large standard deviation, mainly as a result of two samples with amino acid concentrations exceeding 30,000 pmol/mg.

The decrease of the amino acid concentration was especially noticeable in samples taken from the rim area, in which values fell by ~30% in the Neolithic site and ~50% in Mesolithic localities with respect to those of modern specimens. A decrease in the amino acid content in the rim was observed from Mesolithic material to Palaeolithic shells, while this content remained stable in shells from Magdalenian, Solutrean, Gravettian, and Aurignacian sites.

Regarding the concentration of amino acids, [Asx] in the rim and [Glx] in the apex and rim were higher in modern and Neolithic limpets, while they were similar in pre-Neolithic

401 samples (Figs. 4, 5), although [Asx] content in the apex area did not vary significantly with
402 age.

403 Similar percentages were obtained for apex and rim sub-samples for all amino acids
404 (considering [Asx], [Glx], [Ser], [Ile], [Leu], [Phe], [Val], [Ala], Gly], [Arg] and [Thr])
405 However, the percentage of each amino acid varied in a different way with age (Fig. 7). The
406 percentage of Asx increased progressively with age (Fig. 7), i.e. for modern specimens it was
407 around 40%, whereas for the Neolithic ones (Kobaederra) it was 47%, for Mesolithic ones ca.
408 55%, and for Magdalenian, Solutrean, Gravettian and Aurignacian ones 65%. In this regard,
409 samples older than ca. 12,500 cal. yr BP (Upper Magdalenian) and up to ca. 34,000 cal. yr BP
410 showed similar proportions of [Asx]. In contrast, the percentages of Glx, Ala, Phe, Gly and
411 Ile showed a sharp decrease in limpets from modern to the Mesolithic age, after which the
412 percentage of these amino acids remained almost constant in Palaeolithic samples.

413 A rapid decrease was observed in the percentage of [Ser], [Thr], and [Arg] from modern
414 limpets to those of the Mesolithic period, after which the content of these amino acids
415 decreased steadily until ca. 30 ka. This was especially significant in [Ser] (from 10% in
416 modern shells to 2% in Solutrean ones). It should be noted that the percentages of [Val] and
417 [Leu] remained almost the same.

418

419 ***4.1.2 Apex - bleached***

420

421 The concentration of amino acids in the apex of bleached limpets (representing the amino
422 acids that comprise only intra-crystalline proteins) was similar for modern and archaeological

representatives of different ages (Fig. 4). The same results were obtained for [Asx] and [Glx] (Figs. 5, 6).

4.2 Interpretation of amino acid concentration trends

4.2.1 Inter-crystalline amino acids

Significant protein leaching is likely to have occurred from the inter-crystalline fraction during the ca. 6,000 cal. yr after the death of the limpets, as the total amino acid content decreased over this time, and then stabilised. After this decrease, the amino acid content in limpets of Mesolithic and Palaeolithic ages (up to ca. 34 cal. ka BP) remained almost the same (Fig. 4), whereas the contribution of each amino acid to the total content differed (Fig. 7). However, [Asx] in the apex area of archaeological shells did not differ significantly with respect to modern ones.

Also, there was an increase in the percentage of [Asx] in both apex and rim areas with age. The percentages of other amino acids such as Glx, Ala, Phe, Gly and Ile decreased with age. This observation might be explained by the position of each amino acid in the protein chains, thus producing different degradation rates (Kriausakul and Mitterer, 1980; Mitterer and Kriausakul, 1984; Wehmiller, 1980, 1993).

4.2.2 Intra-crystalline amino acids

444

445 The intra-crystalline proteins represented around 15% with respect to the total proteins in
446 modern *Patella* shells (Fig. 4). This percentage increased with age (up to 20–30% over 34
447 ka), in spite of the apparently limited degradation of the proteins in this fraction (the
448 concentration of amino acids remained constant with age in the bleached samples), indicating
449 that there was a preferential break-down and loss of inter-crystalline proteins. Similarly [Asx]
450 and [Glx] also remained constant with age. This finding coincides with reports by Penkman
451 et al. (2008), who observed that the proportion of intra-crystalline amino acids within the
452 whole shell increases as the sample ages.

453 Of note, acidic amino acids represent a high proportion of the fraction with age, as reflected
454 by the increase in the relative percentages of Asx from modern to Palaeolithic shells (Table
455 3).

456 It is also remarkable that while Asx and Glx D/L values differed in the two inter- and intra-
457 crystalline fractions of archaeological limpets, in this case Asx D/L values in intra-crystalline
458 proteins were lower and Glx D/L values were higher than in the inter-crystalline ones (Fig.
459 3), which could be attributable to the removal of certain proteins and amino acids from the
460 inter-crystalline matrix of the shells when bleaching (cf. Penkman et al., 2007, 2008). In this
461 sense, the higher concentration of free amino acids within the intra-crystalline fraction (which
462 are the most highly racemised), may explain the lower Glx D/L values obtained in the inter-
463 crystalline fraction. However, other processes may have to be taken into account, i.e.,
464 different amino acids contribute to the proteins entrapped within the biomineral, which
465 undergo racemisation at different rates (cf. Penkman et al., 2008), and the position of each
466 amino acid in the protein chains can produce different degradation rates (Kriausakul and
467 Mitterer, 1980; Mitterer and Kriausakul, 1984; Wehmiller, 1980, 1993). As evidence here,

the percentage of amino acids differed in bleached and unbleached samples (Table 3). Likewise, partial leaching of the inter-crystalline matrix of proteins may have influenced in the Asx D/L values.

The differences found in the concentration and composition of amino acids and D/L values between inter- and intra-crystalline proteins are in agreement with Sykes et al. (1995) and Penkman et al. (2007, 2008), who observed distinct racemisation rates in these fractions in a variety of mollusc shells. In leaching experiments (140ºC for 24 h to 240 h) on unbleached and bleached *Bithynia* and *Patella* shells, Penkman et al. (2008) and Demarchi et al. (2013a) observed that only a small percentage (1–4%) of the total amino acid content leached from the intra-crystalline fraction, in contrast to a higher percentage (ca. 40%) leached from unbleached shells under the same conditions. While inter-crystalline proteins are more susceptible to decomposition or leaching, the intra-crystalline fraction has been found to approximate a closed system in various mollusc shells. Amino acids within the crystals are apparently effectively isolated from variable external factors, although Orem and Kaufman (2011) observed that the intra-crystalline fraction in the bivalve *Margaritifera* is not a closed system under certain conditions.

5 Aminochronology of limpet shells

5.1 Asx and Glx D/L values vs. age

5.1.1 Apex-unbleached

In general, limpet shells from archaeological sites showed Asx and Glx D/L values consistent with their age (Fig. 3), i.e. in the Neolithic site (Kobaederra) shells had the lowest Asx and Glx D/L values, followed by those belonging to the Mesolithic (level 29 of La Riera, level 1.3 of Mazaculos II, El Penicial, Bricia-A and Arenillas), Azilian/Magdalenian (level 27 of La Riera), Magdalenian (levels 24, 23 and 18.1 of La Riera, Bricia-C, La Lloseta and Les Pedroses), and Aurignacian (El Cuco) periods. However, some exceptions were detected: in level 2/3 of Fuente del Salín (Gravettian), D/L values were similar to those of the Lower Magdalenian sites. Likewise, Solutrean (levels 16, 10 and 8 of La Riera) and Pre-Solutrean (level 1 from La Riera) sites showed lower Asx D/L values than those expected.

5.1.2 Apex-bleached

As with Asx and Glx D/L values of unbleached apex samples, D/Ls also increased with age in the bleached fraction (Fig. 3). Asx D/L values were higher in the unbleached samples, and a strong correspondence (r^2= 0.92) was observed between Asx D/L values of both fractions (Fig. 9). Glx D/L values were slightly higher in bleached Neolithic, Mesolithic, and Upper Palaeolithic shells than those of unbleached samples, being clearly higher in shells from older levels (Fig. 3). Also, a strong correspondence (r^2= 0.85) was found between Glx D/L values of both fractions (Fig. 9).

5.2 Temperature measurement inside the sediment

Fig. 10 shows a plot of the temperature registered at 4-h intervals in the sediment of selected archaeological localities in northern Spain over the course of a year (2013), together with

atmospheric temperature obtained from the meteorological station of Llanes. The monthly and annual mean temperatures measured in the sediment of selected localities during 2013 are shown in Table 4.

Two main considerations are interpreted from the data recorded: 1) atmospheric temperature affects all localities, although its effect is less marked inside the sediment (10-15 cm deep) at the entrance of the caves (no more than 3 m far from the entrance), and variations are attenuated; and 2) temperature within the sediment differs between caves. The archaeological remains of Mazaculos II, La Riera, Bricia, El Penicial and La Lloseta are currently preserved at lower temperatures than at other sites, while at El Cuco, temperatures are significantly higher than at the other sites, probably because it is oriented to the south.

5.3 Aminochronological considerations

A general increase between Asx D/L values and radiocarbon ages was observed (Fig. 3) up to 18 cal. ka. We propose that the palaeoclimatic variations occurred after the accumulation of the archaeological remains affected the amino acid racemization rate of *P. vulgata*- shells, as it was observed that atmospheric temperature affects sediments bearing the limpets in the entrance of the caves. Levels belonging to the Solutrean (levels 16 to 1 of La Riera) and Gravettian (level 2/3 of Fuente Salín) periods showed lower Asx D/L values than expected, but similar values to those typical of Magdalenian localities (Fig. 3). During the Last Glacial Maximum (LGM), temperatures in the sediment would have been lower than during the Holocene, i.e., according to Bard (2002) and Peck et al. (2008), sea surface temperature in the North Atlantic during the LGM was 5-6ºC lower than during the Holocene, thus decreasing the racemisation rate. This is especially noticeable at La Riera, where Asx D/L values of

shells in the Asturian, Azilian/Magdalenian, Magdalenian levels were in agreement with calibrated ^{14}C ages and the periods to which they belong (Fig. 3). In contrast, limpets in the Solutrean and Pre-Solutrean levels showed lower Asx D/L values than expected (Fig. 3), and probably those of Lower Magdalenian as well. As we observed, the main leaching of open-system proteins occurred during the first 6,000 yr after the death of the limpets (Fig. 4). As temperature influences the racemisation rates of amino acids, the low temperatures that occurred during the Last Glaciation appears to have slowed the racemisation of limpets from 27,000 cal. yr BP to at least 18,000 cal. yr BP, after which they followed a similar rate to that of shells in Magdalenian levels (18,000-12,000 cal. yr BP). This explanation could account for the observation that limpets from the Solutrean and Gravettian levels showed lower Asx D/L values than those expected, with an apparent decrease in racemisation between 18-27 cal ka BP i.e, both in unbleached and bleached apex of limpets (Fig. 3).

It is noticeable that the El Cuco samples, deposited under cold conditions, showed significantly higher Asx and Glx D/L values than levels belonging to Solutrean and Gravettian. This may be explained by the orientation of the entrance of this site (to the south), increasing the solar radiation received in comparison with other localities. In support of this, higher temperatures were measured by the loggers (Table 4, Fig. 10), indicating that this site may have not been as affected by the decrease in rates due to cold conditions as the other sites. Nevertheless, other explanations are possible, including that the ^{14}C ages for the El Cuco remains may be in error; it is planned to perform new radiometric dating.

The climate amelioration that occurred from the start of the Late-Glacial and throughout the Holocene explains the general agreement between radiocarbon ages and the aminostratigraphy of Magdalenian, Azilian, Mesolithic and Neolithic levels. However, in

562 some cases there was a discordance, which may be explained by the taphonomical conditions
563 that affected these sites.

564 Of note, level A of Bricia Cave and the shell midden of La Riera (level 29) were dated by ^{14}C
565 at 7,375 ± 185 cal. yr BP and 7,680 ± 150 cal. yr BP (Clark, 1976), respectively, but they
566 showed different mean Asx D/L values (0.264±0.008 for level A of Bricia, and 0.248±0.009
567 for La Riera shell midden-level 29). Although these two caves are less than 100 m apart and
568 positioned on the same karstic massif, they also showed different mean annual temperatures
569 over the year recorded. La Riera Cave experienced lower temperatures, especially noticeable
570 during the summer months, in which a mean difference of 3ºC was observed, whereas during
571 winter, temperatures differed by less than 1ºC. Glx D/L values were only slightly higher in
572 BRI-A (0.089±0.004) than in RIE-29 (0.081±0.005), which is explained by the lower
573 racemisation rate of Glx in comparison with that of Asx.

574 Likewise, the mean Asx D/L value in Arenillas rock-shelter was higher than expected, as the
575 shell midden remains were dated at 6,385±70 cal. yr BP (Bohígas and Muñoz, 2002**)**. In this
576 case, the mean annual temperature was observed to be higher (3-4ºC) than in other localities
577 of similar age (Fig. 10), explaining the Asx D/L values. In addition, recent radiocarbon dating
578 has indicated that these deposits accumulated ca. 7,800 cal. yr BP (unpublished data).
579 However, the effects of other factors in elevating the D/Ls cannot be ruled out.

580 This study indicates that Asx D/L and Glx D/L provide a useful method for dating limpets
581 from archaeological levels younger than ca. 18 cal. ka BP in this region. For older sites (at
582 least those belonging to the Gravettian and Solutrean which were formed under cold
583 climates), past temperatures are likely to have decreased racemisation rates, and extrapolation
584 of Asx D/L values to age should therefore take this into account. Likewise, taphonomical and
585 environmental conditions must be considered in all sites for accurate age estimation.

6. Conclusions

In summary:

1.-Amino acid D/L values in the apex (M+3 and M+2 layers) and rim (M-2 layer) areas of unbleached *P. vulgata* shells are comparable and can therefore both be used for the age calculation of archaeological localities. These zones are made of the same polymorph of calcium carbonate (calcite). In contrast, D/L values in the aragonitic intermediate area (M+1, M and M-1 layers) are higher.

2.-Proteins in rim and apex areas are probably similar, as the percentages of amino acids within them contribute the same percentage to the total amino acid content and vary in the same way with increasing age. Nevertheless, higher amounts of amino acids were found in the rim of modern limpet shells than in the apex, although in archaeological ones, similar concentrations were observed.

3.-The main leaching of open-system proteins in *P. vulgata* shells (at least the inter-crystalline fraction) occurred within the first 6,000 cal. yr BP after the death of the organism. This is evidenced by the considerable decrease in the total amino acid content in Mesolithic samples with respect to modern and Neolithic ones. However, leaching may be faster, as limpets from the Neolithic Kobaederra-2 site showed high variability in the concentrations and percentages of amino acids with respect to those of modern ones. However, the total amount of amino acids in the intra-crystalline fraction remained virtually intact for at least 34 ka.

4.-[Asx] remained constant with age (over ca. 34 cal ka BP), both in inter- and intra-crystalline proteins. While the contribution of [Asx] to the total amino acid content was higher in the former, in both fractions it increased with age. The percentage of Asx increased with age in unbleached shells: from 42% in modern limpets to 47% in Neolithic, 55% in Mesolithic, and 65% in Magdalenian, Solutrean, Gravettiean and Aurignacian representatives. The contribution of Asx to the total amino acid content in bleached shells also increased with age (over ca. 34 cal ka BP), although percentages varied. In contrast, the concentration of other amino acids decreased with age ([Glx], [Ser], [Ala], [Phe], [Ile], [Gly], [Thr] and [Arg]), whereas the percentage of [Val] and [Leu] remained almost constant.

5.-Differences in amino acids that contribute to the inter- and intra-crystalline proteins, which undergo racemisation at different rates, may be produced because the products of diagenesis are likely to remain in the intra-crystalline fraction. Likewise, the preferential removal of certain proteins and amino acids from the inter-crystalline matrix through time, might produce that the inter-crystalline protein fraction degraded faster than the intra-crystalline one. Although Asx D/L values were higher in unbleached samples, there was good correspondence between Asx D/L values in inter- and intra-crystalline proteins. However, other amino acids, such as Glx, showed lower levels of racemisation in the inter-crystalline proteins, at least in the first ca. 12,000 cal yr. In our view, it is sufficient to analyse unbleached samples to establish the age of archaeological levels, but bleaching provides important information and complements the interpretation obtained from the inter-crystalline fraction.

6.-Atmospheric temperature affects the sediment bearing the archaeological remains and thus contributes to the rate of AAR of *P. vulgata*, thus explaining why the Gravettian and

631 Solutrean localities, formed during cold conditions, showed D/L values similar to those of
632 Magdalenian ones.

633

634 **Acknowledgements**

635

636 This paper was made possible by funding from the Spanish Ministry of Science and
637 Innovation projects: HAR2010-22115-C02-01 “La respuesta humana al cambio climático
638 global en una zona litoral: el caso del tránsito al Holoceno en la costa cantábrica (10000-5000
639 cal BC)”, and HAR2010-22115-C02-02 “Aplicación del análisis de sustancias orgánicas e
640 inorgánicas a la reconstrucción paleoambiental, cronológica y tafonómica de yacimientos
641 arqueológicos del Norte de España”. We would like to thank the Museo de Prehistoria y
642 Arqueología de Cantabria, Museo y Centro de Investigación de Altamira, Museo de
643 Prehistoria de Asturias for facilitating the access to the archaeological material. We also
644 thank the “Agencia Estatal de Meteorología” of Spain for facilitating the hourly temperatures
645 of selected meteorological stations from Northern Spain. We thank Kirsty Penkman and an
646 anonymous reviewer for their valuable and helpful comments on the manuscript.

647

648 **References**

649

650 Álvarez-Fernández, E., 2011. Humans and marine resource interaction reappraised:
651 Archaeofauna remains during the late Pleistocene and Holocene in Cantabrian Spain, Journal
652 of Anthropological Archaeology 30, 327-343.

Bailey, G. N., Craighead, A. S., 2003. Late Pleistocene and Holocene coastal paleoeconomies: a reconsideration of the molluscan evidence from Northern Spain. Geoarchaeology: An International Journal 18 (2), 175-204.

Bard, E. 2002. Climate shock: abrupt changes over millenial time scales. Physics Today 55, 32-38.

Bateman, M.D., Carr, A.S., Murray-Wallace, C.V., Roberts, D.L., Holmes, P.J., 2008. A dating intercomparison study on Late Stone Age coastal midden deposits, South Africa. Geoarchaeology 23, 715-741.

Bohígas, R., Muñoz Fernández, E., 2002. Excavaciones arqueológicas de urgencia en el Covacho de Arenillas (Isalares, Castro Urdiales) 1992. In: Ontañón, R. (Ed.), Actuaciones Arqueológicas en Cantabria 1987-1999. Arqueología de Gestión, Gobierno de Cantabria, Santander, 45-47.

Carroll, M., Kowalewski, M., Simões, M.G., Goodfriend, G.A., 2003 Quantitative estimates of time-averaging in terebratulid brachiopod shell accumulations from a modern tropical shelf. Paleobiology 29, 381-402.

674 Clark, G.A., 1976. El Asturiense Cantábrico. Bibliotheca Prehistórica Hispana XIII, Madrid.

675

676 Cohen, A.L., Branch, G.M., 1992. Environmentally controlled variation in the structure and
677 mineralogy of Patella granularis shells from the coast of southern Africa: implications for
678 palaeotemperature assessments. Palaeogeography, Palaeoclimatology, Palaeoecology 91, 49-
679 57.

680

681 Davies, D.J., Powell, E.N., Stanton, R.J., 1989. Relative rates of shell dissolution and net
682 sediment accumulation – a commentary: can shell beds form by the gradual accumulation of
683 biogenic debris on the sea floor?. Lethaia 27, 207-212.

684

685 Demarchi, B., Williams, M.G., Milner, N., Russell, N., Bailey, G.N., Penkman, K.E.H., 2011.
686 Amino acid racemization dating of marine shells: a mound of possibilities. Quaternary
687 International 239 (1-2), 114-124.

688

689 Demarchi, B., Rogers, K., Fa, D.A., Finlayson, C.J., Milner, N., Penkman, K.E.H., 2013a.
690 Intra-crystalline protein diagenesis (IcPD) in *Patella vulgata*. Part I: Isolation and testing of
691 the closed system. Quaternary Geochronology 16, 144-157.

692

693 Demarchi, B., Collins, M.J., Tomiak, P.J., Davies, B.J., Penkman, K.E.H., 2013b. Intra-
694 crystalline protein diagenesis (IcPD) in *Patella vulgata*. Part II: Breakdown and temperature
695 sensitivity. Quaternary Geochronology, 158-172.

Fenger, T., Surge, D., Schöne, B., Milner, N., 2007. Schlerochronology and geochemical variation in limpet shells (Patella vulgata): A new archive to reconstruct coastal sea surface temperature. Geochemistry, Geophysics, Geosystems 8 (7), Q07001, doi:10.1029/2006GC001488.

Glover, E., Glover, I., Vita-Finzi, C., 1990. First-order 14C dating of marine molluscs in archaeology. Antiquity 64, 562-567.

González-Morales, M.R., 1982. El Asturiense y otras Culturas Locales. Monografías del Centro de Investigación y Museo de Altamira, Santander.

Gotliv, B.A., Kessler, N., Sumerel, J.L., Morse, D.E., Tuross, N., Addadi, L., Weiner, S., 2005. Asprich: a novel aspartic acid-rich protein family from the prismatic shell matrix of the bivalve *Atrina rigida*. Chem Bio Chem 6, 304–314.

Gutiérrez Zugasti, F. I., 2009. La explotación de moluscos y otros recursos litorales en la región cantábrica durante el Pleistoceno final y el Holoceno inicial. PUbliCan, Ediciones de la Universidad de Cantabria, Santander.

716 Gutiérrez Zugasti, F. I., 2011. Coastal resource intensification across the Pleistocene-
717 Holocene transition in Northern Spain: evidence from shell size and age distributions of
718 marine gastropods. Quaternary International 244, 54-66.

719

720 Haugen, J.E., Sejrup, H.P., 1992. Isoleucine epimerization kinetics in the shells of *Arctica*
721 *islandica*. Norsk Geologisk Tidsskrift 72, 171-180.

722

723 Hearty, P.J., O´Leary, M.J., Kaufman, D.S., Page, M.C., Bright, J., 2004, Amino acid
724 geochronology of individual foraminifer (Pulleniatina obliquiloculata) tests, north Queenland
725 margin, Australia: a new approach to correlating and dating Quaternary tropical marine
726 sediment cores. *Paleoceanography*, **19**, PA4022, doi:10.1029/2004PA001059.

727

728 Hernández-Pacheco, F., Llopis-Lladó, N., Jordá-Cerdá, F., Martínez, J.A., 1957. Libro Guía
729 de la Excursión N2. El Cuaternario de la Región Cantábrica 28-29. Diputación Provincial de
730 Asturias, Oviedo.

731

732 Jordá, F., 1954. La cueva de Bricia (Asturias). Boletín del Instituto de Estudios Asturianos
733 XXII, 169-195.

734

735 Jordá, F., 1957. Prehistoria de la Región Cantábrica. Diputación Provincial de Asturias,
736 Servicio de Investigaciones Arqueológicas, Oviedo.

737

738 Jordá, F., 1958. Avance al estudio de La Lloseta (Ardines, Ribadesella, Asturias). Memorias
739 del Servicio de Investigaciones Arqueológicas de Asturias 3, Oviedo.
740
741 Kaufman, D.S., 2000, Amino acid racemization in ostracodes. In: Goodfriend, G., Collins,
742 M., Fogel, M., Macko, S., Wehmiller, J. (Eds.), Perspectives in Amino Acid and Protein
743 Geochemistry. Oxford University Press, New York, pp. 145-160.
744
745 Kaufman, D.S., Manley, W.F., 1998. A new procedure for determining DL amino acid ratios
746 in fossils using reverse phase liquid chromatography. Quaternary Geochronology 17, 987-
747 1000.
748
749 Kidwell, S.M., 1998. Time-averaging in the marine fosils record: overview of strategies and
750 uncertainties. Geobios 30 (7), 977-995.
751
752 Kidwell, S.M., Best, M.M.R., Kaufman, D.S., 2005. Taphonomic trade-offs in tropical
753 marine death assemblages: Differential time-averaging, shell loss, and probable bias in
754 siliciclastic vs. carbonate facies. Geology 33, 729-732.
755
756 Kosnik, M.A., Kaufman, D.S., 2008. Identifying outliers and assessing the accuracy of
757 amino acid racemization measurements for geochronology: II. Data screening. Quaternary
758 Geochronology 3, 328-341.
759

760 Kriausakul, N., Mitterer, R.M., 1980. Some factors affecting the epimerization of isoleucine
761 in peptides and proteins. In: Hare, P.E., Hoering, T.C., King, J. Jr. (Eds.), Biogeochemistry of
762 amino acids. Wiley, New York, pp. 283-296.
763
764 MacClintock, C., 1967. Shell Structure of Patelloid and Bellerophontoid Gastropods
765 (Mollusca). Peabody Museum of Natural History, Yale University, New Haven.
766
767 Marie, B., Jackson, D.J., Ramos-Silva, P., Zanella-Cléon, I., Guichard, N., Marin, F., 2013.
768 The shell-forming proteome of Lottia gigantea reveals both deep conservations and lineage-
769 specific novelties. The FEBS Journal 280, 214-232.
770
771 Marin, F., Luquet, G., 2004. Molluscan shell proteins. Comptes Rendus Palevol 3, 469-492.
772
773 Marin F., Leroy N., Silva P., Marie B., 2012. The formation and mineralization of mollusc
774 shell. Frontiers in Bioscience, 4, 1099-1125.
775
776 Maroto, J., Vaquero, M., Arrizabalaga, A., Baena, J., Baquedano, E., Jordá, J., Julià, R.,
777 Montes, R., Van Der Plicht, J., Rasines, P., Wood, R., 2012. Current issues in late Middle
778 Palaeolithic chronology: New assessments from Northern Iberia. Quaternary International
779 247, 15-25.
780

Masters, P., Bada J.L., 1977. Racemization of isoleucine in fossil molluscs from Indian middens and interglacial terraces in southern California. Earth and Planetary Science Letters 37, 173-183.

Meldahl, K.H., Flessa, K.W., Cutler, A.H., 1997. Time-averaging and postmortem skeletal survival in benthic fossil assemblages: quantitative comparisons among Holocene environments. Paleobiology 23, 209-229.

Mitterer, R.M., Kriausakul, N., 1984. Comparison of rates and degrees of isoleucine epimerization in dipeptides and tripeptides. Organic Geochemistry 7, 91-98.

Moure, A., González Morales, M.R., 1992. Datation 14C d'une zone décorée de la grotte Fuente del Salín en Espagne. INORA 3, 1-2.

Muñoz Fernández, E., Rasines Del Río, P., Santamaría Santamaría, S., Morlote Expósito, J.M., 2007. Estudio arqueológico del abrigo del Cuco. In: Muñoz Fernández, E., Montes Barquín, R. (Eds.), Intervenciones arqueológicas en Castro Urdiales, tomo III. Arqueología y arte rupestre paleolítico en las cavidades de El Cuco o Sobera y La Lastrilla. Excmo. Ayuntamiento de Castro Urdiales, Concejalía de Medio Ambiente y Patrimonio Arqueológico, Castro Urdiales (Spain), pp. 15-160.

Murray-Wallace, CV., 1995. Aminostratigraphy of Quaternary coastal sequences in southern Australia an overview. Quaternary International 26, 69-86.

Murray-Wallace CV, Goede A., 1995. Aminostratigraphy and electron spin resonance dating of Quaternary coastal neotectonism in Tasmania and the Bass Strait islands. Australian Journal of Earth Sciences 42, 51-67.

Orem, C., Kaufman, D.S., 2011. Effects of basic pH on amino acid racemization and leaching in freshwater mollusk shell. Quaternary Geochronology 6, 233-245.

Ortiz, J.E., Torres, T., González-Morales, M.R., Abad, J., Arribas, I., Fortea, F. J., García-Belenguer, F., Gutiérrez-Zugasti, I., 2009a. The aminochronology of man-induced shell middens in caves in Northern Spain. Archaeometry 51, 123-139.

Ortiz, J.E., Torres, T., Delgado, A., Reyes, E., Díaz-Bautista, A., 2009b. A review of the Tagus river tufa deposits (central Spain): age and palaeoenvironmental record. Quaternary Science Reviews 28, 947- 963.

Peck, V.L., Hall, I.R., Zahn, R., Elderfield, H., 2008. Millennial-scale surface and subsurface paleothermometry from the northeast Atlantic, 55–8 ka BP. Paleoceanography 23, PA3221, doi:10.1029/2008PA001631.

Penkman, K.E.H., Preece, R.C., Keen, D.H., Maddy, D., Schreve, D.S., Collins, M.J., 2007. Testing the aminostratigraphy of fluvial archives: the evidence from intra-crystalline proteins within freshwater shells. Quaternary Science Reviews 26, 2958-2969.

827

828 Penkman, K.E.H., Kaufman, D.S., Maddy, D., Collins, M.J., 2008. Closed-system behaviour
829 of the intra-crystalline fraction of amino acids in mollusk shells. Quaternary Geochronology
830 3, 2-25.

831

832 Sarashina, I., Endo, K., 2001. The complete primary structure of Molluscan Shell Protein 1
833 (MSP-1), an acidic glycoprotein in the shell matrix of the scallop *Patinopecten yessoensis*,
834 Marine Biotechnology 3, 362–369.

835

836 Stein, J.K., Deo, J.N., 2003. Big sites-short time. Accumulation rates in archaeological sites.
837 Journal of Archaeological Science 30, 297-316.

838

839 Straus, L.G., Clark, G. A.. 1986. La Rieva cave. Stone Age Hunter-Gatherer Adaptations in
840 Northern Spain. Arizona, Anthropological Research Papers, 36, Arizona State University.

841

842 Straus, L.G., Bernaldo de Quirós, F., Cabrera, V., Clark, G. A., 1978. Solutrean Chronology
843 & Lithic Variability in Vasco-Cantabrian Spain. Zephyrus 28-29, 109-113.

844

845 Sykes, G.A., Collins, M.J., Walton, D.I., 1995. The significance of a geochemically isolated
846 intracrystalline fraction within biominerals. Organic Geochemistry 23, 1059–1065.

847

Torres, T., Llamas, J., Canoira, L., García-Alonso, P., García-Cortés, A., Mansilla, H., 1997. Amino acid chronology of the Lower Pleistocene deposits of Venta Micena (Orce, Granada, Andalusia, Spain). Organic Geochemistry 26, 85-97.

Torres, T., Llamas, J.F., Canoira, L., García Alonso, P., Coello, F.J., 1999. Variaciones intraconcha e interconcha de la racemización del ácido aspártico en moluscos holocenos del Golfo de Cádiz (SO de España). Geogaceta 26, 111-114.

Torres, T., Ortiz**,** J.E., Arribas, I., 2013. Variations in racemization/epimerization ratios and amino acid content of *Glycymeris* shells in raised marine deposits in the Mediterranean realm. Quaternary Geochronology 16, 35-49.

Vega del Sella, C. 1914. La Cueva del Penicial (Asturias). Comisión de Investigaciones Paleontológicas y Prehistóricas 4, Madrid.

Watabe, M., 1984. Shell. In: Bereiter-Hahn, J., Matolsy, A.G., Richards, K.S. (Eds.), The biology of the integument 1. Invertebrates. Springer, Berlin, pp.448-485.

Wehmiller, J.F., 1977. Amino acid studies of the Del Mar, California, midden site-Apparent rate constants, ground temperature models, and chronological implications. Earth and Planetary Science Letters 37, 184-196.

870 Wehmiller, J.F., 1980. Intergeneric differences in apparent racemization kinetics in mollusks
871 and foraminifera: implications for models of diagenetic racemization. In: Hare, P.E., Hoering,
872 T.C., King, K.Jr. (Eds.), Biogeochemistry of amino acids. John Willey and Sons, New York,
873 pp. 341-355.

874

875 Wehmiller, J. F., 1984. Interlaboratory comparison of amino acid enantiomeric ratios in fossil
876 mollusks. Quaternary Research 22, 109-120.

877

878

879 Wehmiller, J., 1990. Amino acid racemization: application in chemical taxonomy and
880 chronostratigraphy of Quaternary fossils. In: Carter, J.G. (Ed.), Skeletal biomineralization:
881 patterns, processes and evolutionary trends. Van Nostrand Reinhold, New York, pp. 583-607.

882

883 Wehmiller, J.F., 1993. Applications of organic geochemistry for Quaternary research. In:
884 Engel, M.H., Macko, S.A. (Eds.), Organic Geochemistry. Plenum Press, New York, pp. 755-
885 783.

886

887 Wehmiller, J.F., Miller, G., De Vogel, S., Kaufman, D.S., Bright, J., Murray-Wallace, C.V.,
888 Ortiz, J.E., Penkman, K., 2010. Interlaboratory comparison of amino acid D/L values.
889 Geological Society of America Annual Meeting, Denver, Abstracts with Programs 42(5), 86.

890

Zapata Peña, L., Ibáñez Estévez, J.J., González Urquijo, J., 1997. El yacimiento de la cueva de Kobaederra (Oma, Kortezubi, Bizkaia). Resultados preliminares de las campañas de excavación 1995-97. Munibe (Antropologia-Arkeologia) 49, 51-63.

896 **Figure captions**

897

898 Figure 1. Geographical location of the caves studied. 1-Kobaederra, 2-El Cuco, 3-Arenillas,
899 4-Fuente Salín, 5-Mazaculos II, 6-Riera, 7-Cueto La Mina, 8-Bricia, 9-Penicial, 10-Lloseta,
900 and 11-Les Pedroses. Cue beach and Llanes meteorological station were also plotted.

901

902 Figure 2. Microphotographs of thin sections of *P. vulgata* shells treated with Feigl's (A-B)
903 and Mutvei's (C to F) solution (Feigl´s solution stained aragonite crystals black, while calcite
904 ones remain unstained; Mutvei's solution stained organic matrix laminae and crystal
905 envelopes in shades of blue). A- cross section of a shell showing the unstained apex area in
906 the central part and the intermediate region stained in black; B- transition between the stained
907 aragonitic intermediate part (M-1, M, M+1 layers) to the unstained rim area (M+2, M+3); C-
908 apex with the M-2 layer with an irregular/radial crossed-lamellar pattern and the transition to
909 the M-1 layer (major growth lines are marked with arrows) stained in blue; D- contact
910 between the intermediate part (M-1, M+1) with a complex crossed-lamellar structure and the
911 rim (M+2, M+3 layers) with a concentric crossed-lamellar pattern (major growth lines are
912 marked with arrows); E- detail view of the rim area (M+2, M+3 layers) and the M+1, M, and
913 M-1 layers (minor growth lines are marked with arrows); F- detailed view of the rim area
914 (M+2, M+3 layers), which shows a concentric crossed-lamellar pattern, the aragonitic M+1
915 layer, which shows complex crossed-lamella, and the M layer, which shows a prismatic
916 structure with large crystals oriented perpendicular to the shell surface; G- detailed view of
917 the complex crossed-lamellar structure of the M-1 layer; H- detailed view of the concentric
918 crossed-lamellar structure of the M+2 layer.

Figure 3. Relationship between age (cal. yr BP) of archaeological sites and mean Asx and Glx D/L values for unbleached apex and rim and bleached apex samples of *Patella* shells (data shown in Table 2-Supplementary information). Dashed lines indicate estimated racemisation patterns for Asx in unbleached and bleached apex samples .

Figure 4. Relationship between age (cal. yr BP) of archaeological sites and the total amino acid content in bleached and unbleached apex and unbleached rim of *Patella* shells (data shown in Table 3-Supplementary information).

Figure 5. Relationship between age (cal. yr BP) of archaeological sites and the Asx content in bleached and unbleached apex and unbleached rim of *Patella* shells (data shown in Table 4-Supplementary information).

Figure 6. Relationship between age (cal. yr BP) of archaeological sites and the Glx content in bleached and unbleached apex and unbleached rim of *Patella* shells (data shown in Table 4-Supplementary information).

Figure 7. Percentage of each amino acid in the unbleached apex (A) and rim (B) areas of *P. vulgata* shells from modern and archaeological sites. The same colour code was used for all the levels of the same period, and localities are plotted in age order indicated in the legend.

940

941 Figure 8. Percentage of each amino acid concentration in the apex, rim and intermediate areas
942 of modern *P. vulgata* shells (data shown in Table 5-Supplementary information).

943

944 Figure 9. Comparison of Asx D/L and Glx D/L values in bleached and unbleached samples
945 from the apex of *P. vulgata* shells of different ages.

946

947 Figure 10. Annual temperature record of the sediment in some archaeological localities
948 compared to the atmospheric temperature recorded in the meteorological station of Llanes
949 during 2013.

950

951 Figure 1-Supplementary Data. Chromatogram showing the D and L peaks of the following
952 amino acids: aspartic acid and asparagine (Asx), glutamic acid and glutamine (Glx), serine
953 (Ser), alanine (Ala), valine (Val), phenylalanine (Phe), isoleucine (Ile), leucine (Leu),
954 threonine (Thr), arginine (Arg), and tyrosine (Tyr), together with the abundance of glycine
955 (Gly).

956

957 Figure 2-Supplementary Data. Comparison between D/L values obtained by gas-
958 chromatography (GC) and high performance liquid chromatography (HPLC) in the
959 Biomolecular Stratigraphy Laboratory for A) Asp and B) Glu in the same samples. Based on
960 the data of Table 4 of Ortiz et al. (2009b).

961

962 Figure 3-Supplementary Data. Best-fit exponential relation between Asx D/L versus Glx D/L
963 values obtained in the unbleached apex of *Patella* shells. Each subsample is represented by a
964 black dot, and outliers are in red with the laboratory (LEB) number. The best-fit regression is
965 plotted.

966

967 Figure 4-Supplementary Data. Best-fit exponential relation between Asx D/L versus Glx D/L
968 values obtained in the unbleached rim of *Patella* shells. Each subsample is represented by a
969 black dot, and outliers are in red with the laboratory (LEB) number. The best-fit regression is
970 plotted.

971

972 Figure 5-Supplementary Data. Best-fit exponential relation between Asx D/L versus Glx D/L
973 values obtained in the bleached apex of *Patella* shells. Each subsample is represented by a
974 black dot, and outliers are in red with the laboratory (LEB) number. The best-fit regression is
975 plotted.

976

977 Figure 6-Supplementary Data. Asx D/L values (including outliers- represented in black) in
978 the apex (unbleached and bleached samples) compared to those in the rim area (unbleached
979 samples) of modern and also archaeological *P. vulgata* shells, including mean values
980 (excluding outliers) for each locality. Asx D/L values measured in intermediate parts of
981 modern specimens were also plotted.

982

983 Figure 7-Supplementary Data. Glx D/L values (including outliers- represented in black) in
984 the apex (unbleached and bleached samples) compared to those in the rim area (unbleached

985 samples) of modern and also archaeological *P. vulgata* shells, including mean values
986 (excluding outliers) for each locality. Glx D/L values measured in intermediate parts of
987 modern specimens were also plotted.

988

989

990

991 **Tables**

992 **Table 1. Geographical location of the archaeological levels studied and the periods**
993 **assigned. Calibrated ages (cal yr) were converted using the Radiocarbon Calibration**
994 **Program 7.0 (CALIB 7.0) (Stuiver et al., 2014) with the calibration dataset IntCal13**
995 **(Reimer et al., 2013). Original radiocarbon ages are in Table 1-Supplementary**
996 **information.**

Cave	Latitude	Longitude	Elevation a.s.l. (m)	Archaeological level	Age (cal. yr BP)
Cue beach	43º25´4´´N	4º43´45´´W	0	-	Modern
Kobaederra (KBR)	43º20´35´´N	2º37´3´´W	260	Level 2	Neolithic [1] 5,975±160 (UBAR-472)
Arenillas (ARE)	43º23´44´´N	3º18´46´´W	20	Shell midden	Asturian [2] 6,385±70 (GrN-19596)
Bricia (BRI)	43º25´38.2´´N	4º51´17.8´´W	50	Shell midden (Level A [5]) Level C [5]	Asturian [3,4] 7,680±150 (GaK 2908) Upper Magdalenian [3]
Mazaculos II (MAZ)	43º23´26´´N	4º34´43´´W	35	Shell midden Level 1.3	Asturian [6] 8,490±40 (UGAM-9081)
La Riera (RIE)	43°25′26.86″N	4°50′53.63´´W	35	Shell midden 29 Level 27upper Level 24 Level 23 Level 18.1 Level 16 Level 10 Level 8 Level 1	Asturian [3] 7,375±185 (GaK-3046) Azilian/Magdalenian[7] 12,510±195 (BM-1494); 17,960±490 (GaK-6985) Upper Magdalenian [7] 12,660±545 (GaK-6982) Upper Magdalenian [7] 11,945±730 (Ly-1646) Lower Magdalenian [7] 18,430±530 (Q-2116); 18690±490 (Q-2110); 19,680±555 (GaK-6448) Solutrean [7] 21,750±770 (GaK-6983) Solutrean [7] 23,690±565 (GaK-6447) Solutrean [7] 24810±1055(GaK-6981) 19,090±350 (GaK-6450) Pre-Solutrean [7] 23485±550(UCR-1270) 24285±565 (Ly-1 783); 24,285±525 (BM-1739)
El Penicial (PEN)	43º26´42.9´´N	4º56´22.3´´W	60	Surface shell midden	Asturian [3,8] 9,760±250 (GaK 2906)
Les Pedroses (LPS)	43º27´26.6´´N	5º6´17.7´´W	80	20 cm thick level	Lower Magdalenian [3,9]
La Lloseta (LLO)	43º27´38.3´´N	5º4´29.1´´W	40	Level B (sample A)	Middle Magdalenian [3] 18,340±280 (GaK 2549)
Fuente del Salín (FTS)	43°22´7´´N	4°28´52´´W	10	Level 2/3	Gravettian[10] 26,850±775(GrN-18574) 27,315±385(GX-27756)
El Cuco (CUC)	43°23´28”N	3°13´40”W	25	Level XIII	Aurignacian [11] 34,290±160(GrA 32436)

997 **1.-Zapata Peña et al. (1997) ; 2.-Bohígas and Muñoz (2002) ; 3.-Clark (1976);** 4.**-Jordá (1957, 1958); 5.-**
998 **Jordá (1954); 6.-González Morales (1982); 7.- Straus et al., 1978; Straus and Clark, 1986; 8.-Vega del**
999 **Sella (1914); 9.-Hernández-Pacheco *et al.* (1957); 10.-Moure and González Morales, 1992; 11.-Muñoz**
1000 **Fernández et al. (2007).**

1001
1002

Table 2. Mean total amino acid, Asx, and Glx concentrations (pmol/mg), and Asx D/L and Glx D/L values in unbleached samples taken from the apex, rim, and intermediate areas of modern *P. vulgata* shells.

Area	[total]	[Asx]	[Glx]	Asx D/L	Glx D/L
Apex	25462±6354	10616±3165	1772±355	0.047±0.006	0.026±0.004
Rim	43478±10786	18154±3489	3361±928	0.048±0.001	0.027±0.001
Interm	22384±4592	8669±2132	1793±432	0.112±0.018	0.049±0.004

Table 3. Percentage of Asx and Glx content with respect to the total amino acid content of unbleached and bleached samples taken from the apex area of modern and archaeological *P. vulgata* shells in modern and archaeological localities.

Period	Localities	N	%[Asx] Apex	%[Asx] Apex Bleached	%[Glx] Apex	%[Glx] bleached
	Modern	12	41.1 ± 3.7	23.2 ± 7.0	7.2 ± 1.1	10.6 ± 2.3
N	KBR-2	4	47.1 ± 5.8	26.0 ± 12.7	6.9 ±1.0	12.8±3.0
M	RIE-29	5	56.3 ± 3.1	27.6 ± 2.3	5.7 ± 0.3	9.8 ± 0.6
	ARE	7	58.0 ± 2.7	30.5 ± 6.7	5.8 ± 0.6	12.4 ± 1.9
	BRI-A	5	52.1 ± 5.3	29.6 ± 9.9	7.0 ± 1.3	12.2 ± 3.0
	MAZ II-1.3	9	53.2 ± 7.1	29.8 ± 6.4	6.4 ± 1.6	11.8 ± 1.6
	PEN	5	58.7 ± 0.9	33.0 ± 2.7	5.8 ± 0.1	10.6 ± 2.9
UM	BRI-C	5	59.9 ± 3.2	32.0 ± 3.8	5.7 ± 0.5	9.4 ± 1.1
	RIE-27	5	60.6 ± 1.9	42.9 ± 2.4	5.5 ± 0.4	8.3 ± 0.4
	RIE-24	3	60.4 ± 0.4	42.0 ± 5.1	5.4 ± 0.6	8.9 ± 1.1
	RIE-23	4	61.2 ± 4.6	40.7 ± 3.3	5.7 ± 0.9	9.5 ± 0.5
LM	LLO	5	63.4 ± 2.3	41.0 ± 4.7	5.4 ± 0.3	8.1 ± 0.4
	LPS	5	62.4 ± 3.3	44.1 ± 3.1	6.0 ± 0.7	8.3 ± 0.6
	RIE-18.1	5	64.9 ± 0.3	46.4 ± 4.6	5.3 ± 0.3	8.5 ± 1.0
S	RIE-16	5	63.8 ± 3.5	46.5 ± 2.8	5.1 ± 0.1	8.4 ± 0.6
	RIE-10	5	64.7 ± 1.8	45.8 ± 2.1	5.3 ± 0.2	8.5 ± 0.3
	RIE-8	5	62.7 ± 1.4	41.2 ± 2.5	5.6 ± 0.3	9.3 ± 0.5
	RIE-1	5	64.1 ± 3.2	45.1 ± 2.0	5.5 ± 0.5	8.3 ± 0.5
G	FTS-2/3	7	64.1 ± 0.9	40.9 ± 3.7	5.6 ± 0.2	9.3 ± 1.2
A	CUC	7	66.0 ± 1.3	49.2 ± 2.3	5.8 ± 0.2	8.3 ± 0.3

N:Neotlithic; M: Mesolithic (Asturian); UM: Upper Magdalenian; LM: Lower Magdalenian; S: Solutrean; G: Gravettian; A: Aurignacian.

Table 4. Mean monthly and annual temperature (in degrees Celsius) record in the sediment of some archaeological localities (measured at 4-h intervals).

Cave	Annual	January	February	March	April	May	June	July	August	September	October	November	December
Cuco	17.6	14.2	13.4	15.5	17.2	15.7	16.8	20.8	22.5	22.3	21.1	16.3	14.6
Arenillas	15.2	10.4	9.6	11.5	13.5	13.6	16.2	21.8	22.3	20.4	19.0	13.2	10.9
Mazaculos	11.8	9.0	8.6	8.6	9.6	10.3	12.3	15.3	15.6	14.9	14.2	11.8	8.6
La Riera	11.2	9.6	9.1	9.0	9.7	10.2	11.4	12.8	13.6	13.8	13.6	12.0	9.3
Bricia	12.2	9.5	9.0	9.4	10.3	10.7	12.7	16.5	16.5	15.7	14.8	12.0	9.2
Penicial	11.8	9.2	8.8	8.8	9.9	10.3	12.1	15.3	15.9	15.3	14.6	12.3	9.0
Lloseta	11.0	8.9	8.7	8.5	9.3	9.6	11.4	13.9	14.5	14.2	13.8	11.4	7.8

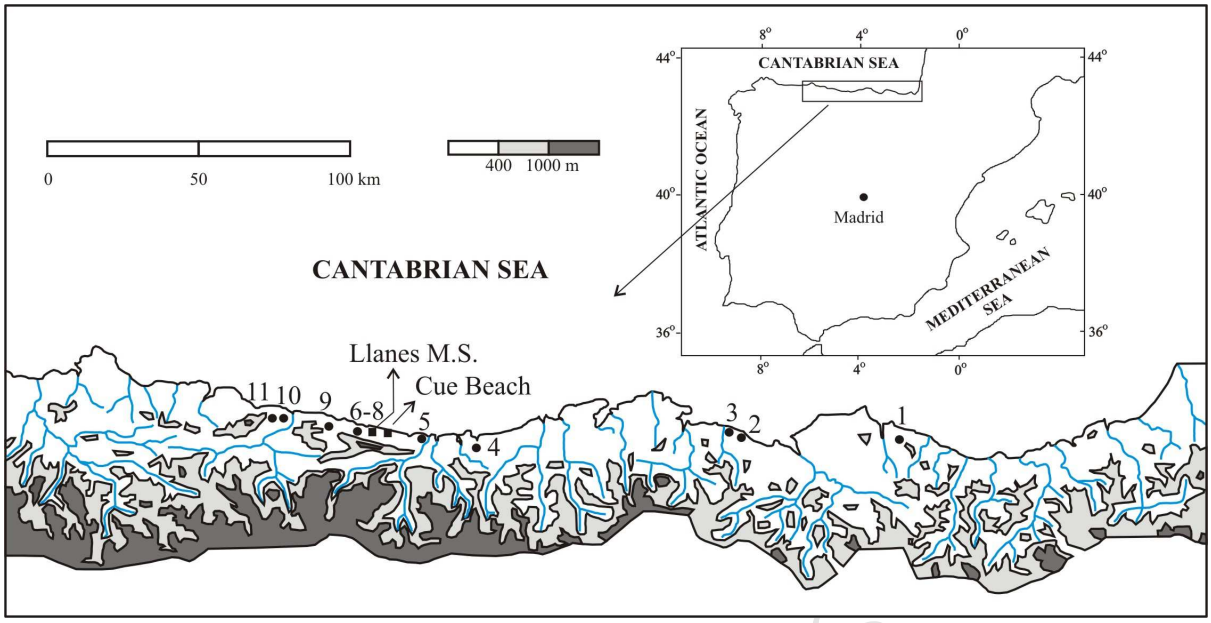

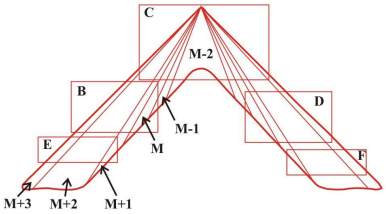

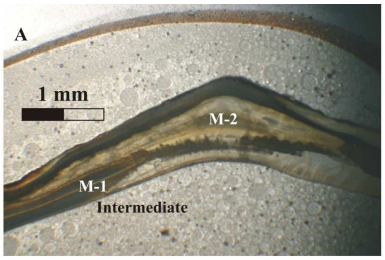

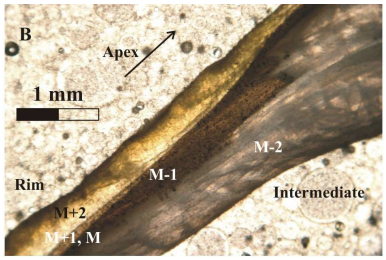

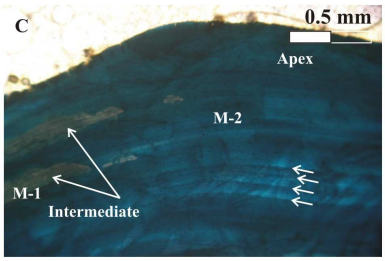

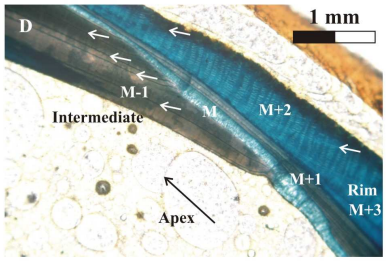

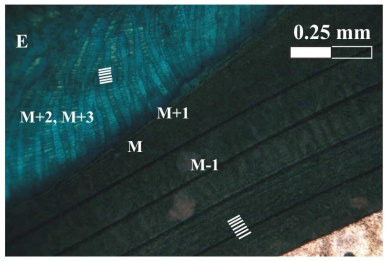

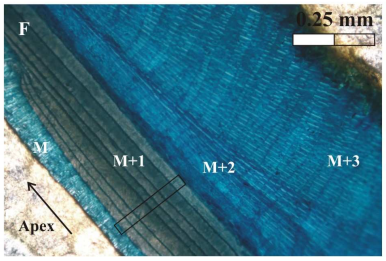

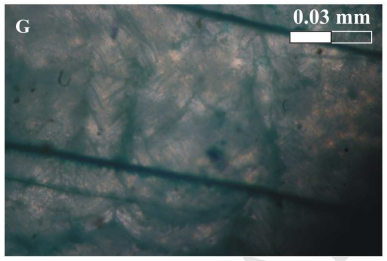

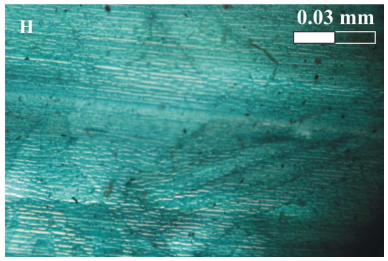

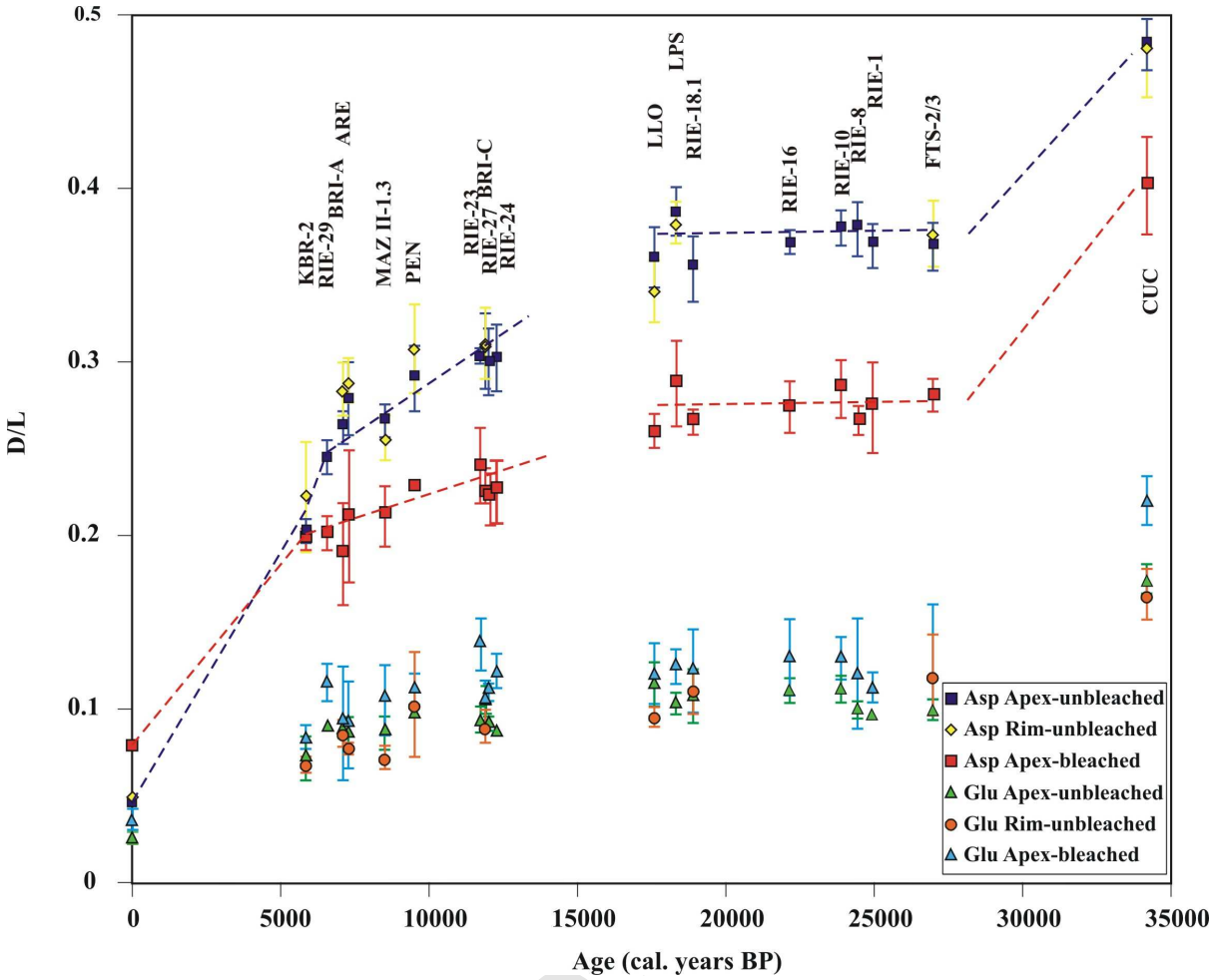

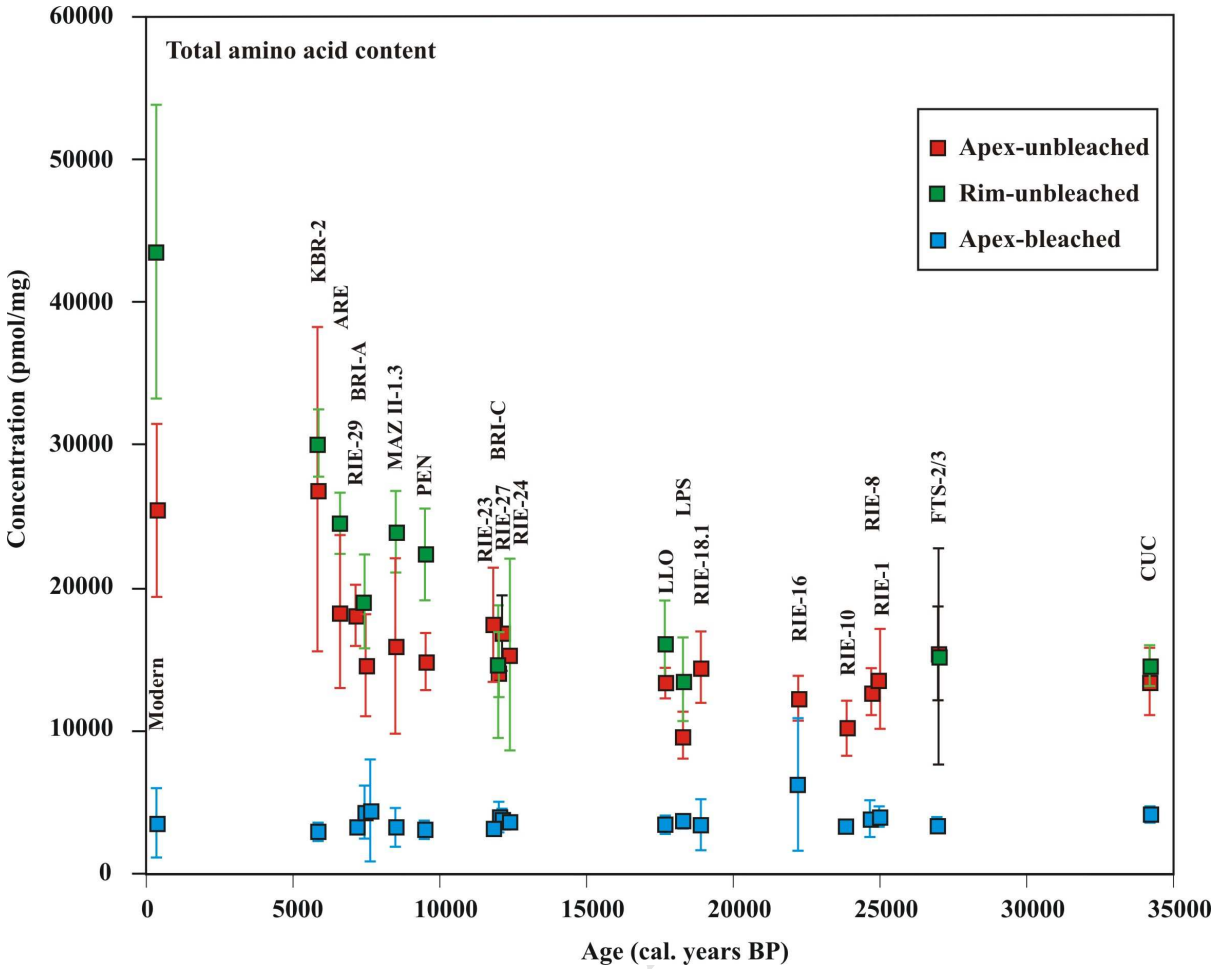

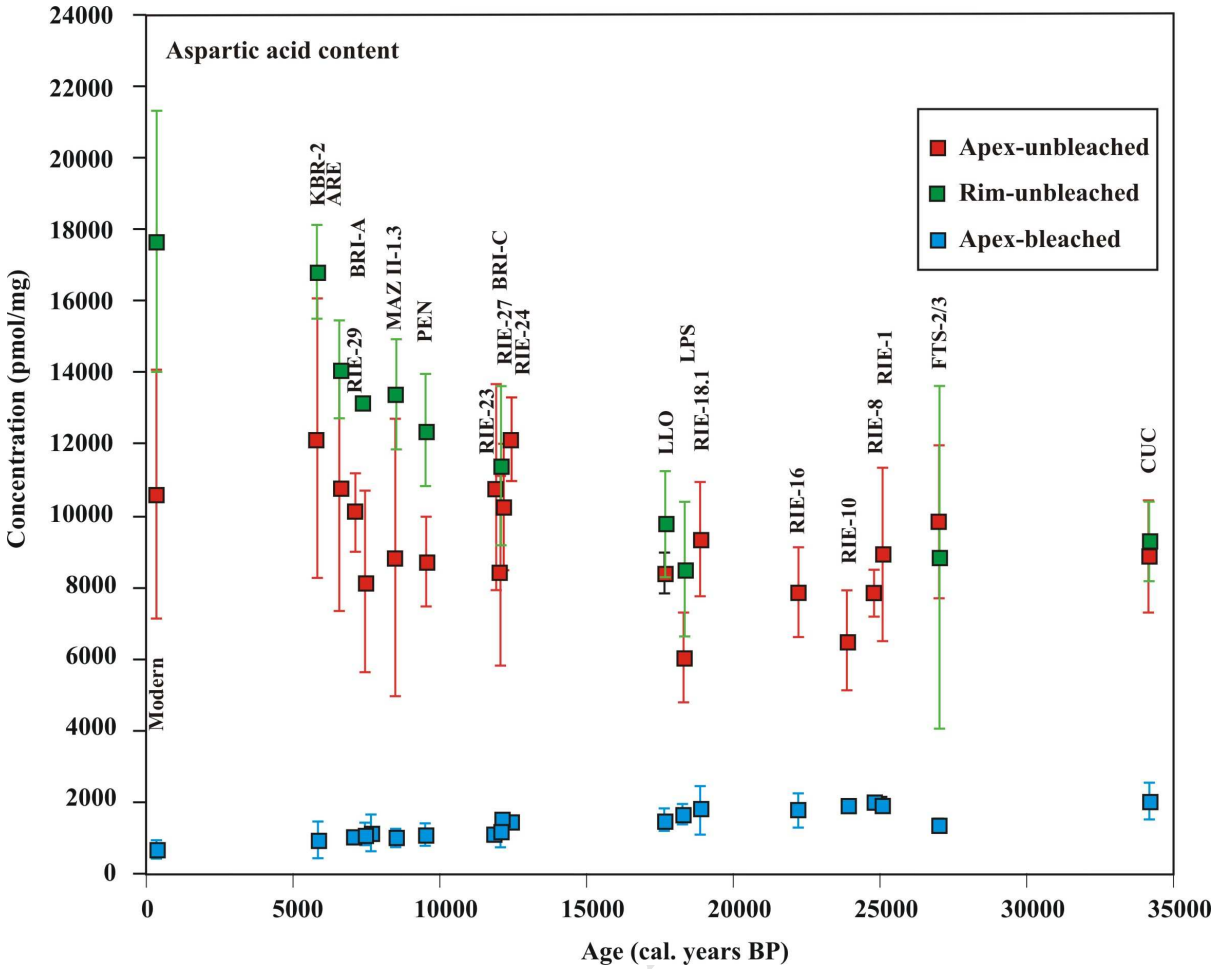

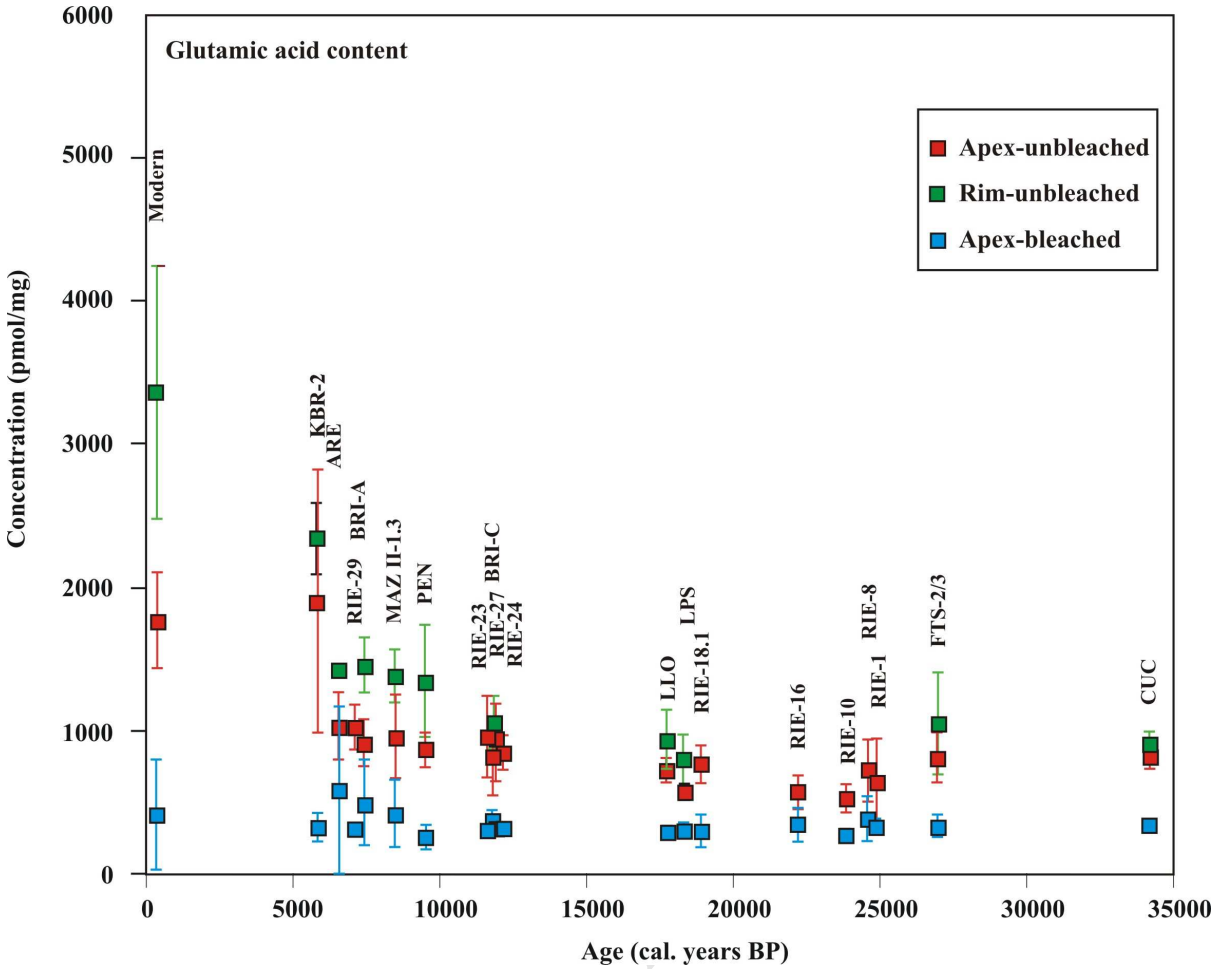

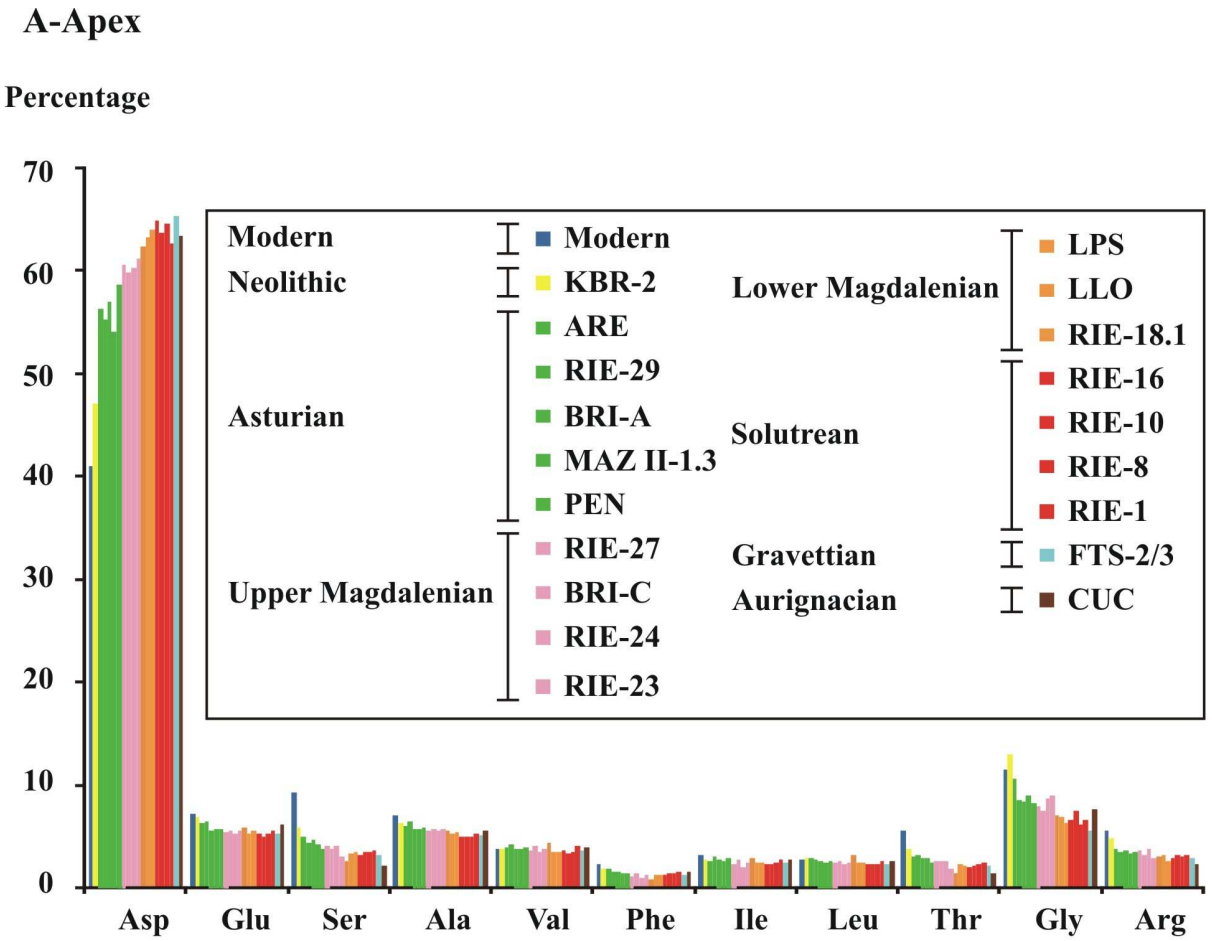
A-Apex
Percentage
70
60
50
40
30
20
10
0
Modern
Neolithic
Asturian
Upper Magdalenian
Modern
KBR-2
ARE
RIE-29
BRI-A
MAZ II-1.3
PEN
RIE-27
BRI-C
RIE-24
RIE-23
Lower Magdalenian
Solutrean
Gravettian
Aurignacian
LPS
LLO
RIE-18.1
RIE-16
RIE-10
RIE-8
RIE-1
FTS-2/3
CUC
Asp
Glu
Ser
Ala
Val
Phe
Ile
Leu
Thr
Gly
Arg

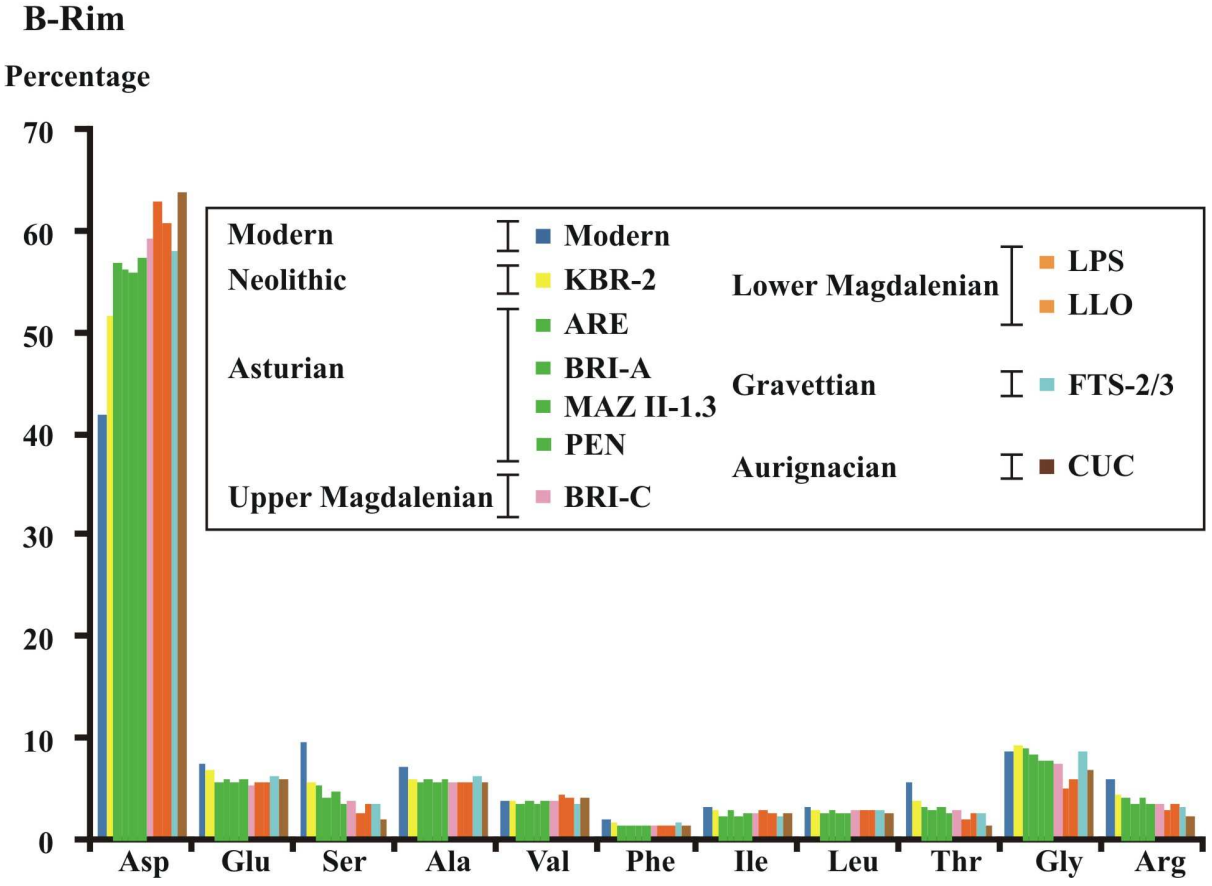
B-Rim
Percentage
70
60
50
40
30
20
10
0
Modern
Neolithic
Asturian
Upper Magdalenian
Modern
KBR-2
ARE
BRI-A
MAZ II-1.3
PEN
BRI-C
Lower Magdalenian
Gravettian
Aurignacian
LPS
LLO
FTS-2/3
CUC
Asp
Glu
Ser
Ala
Val
Phe
Ile
Leu
Thr
Gly
Arg

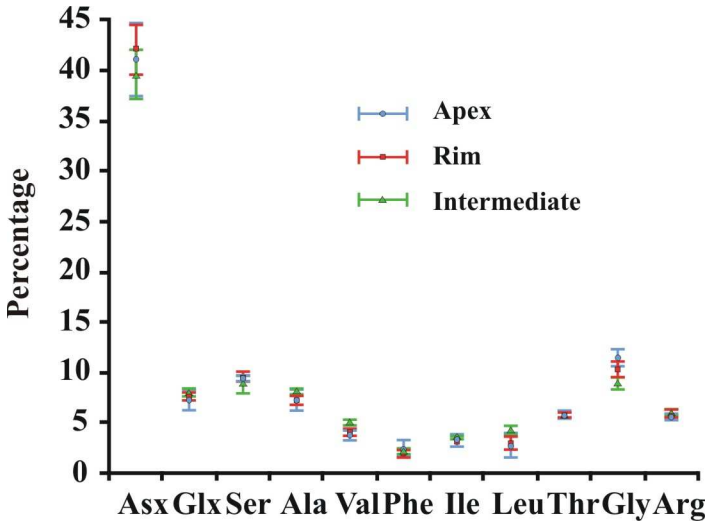

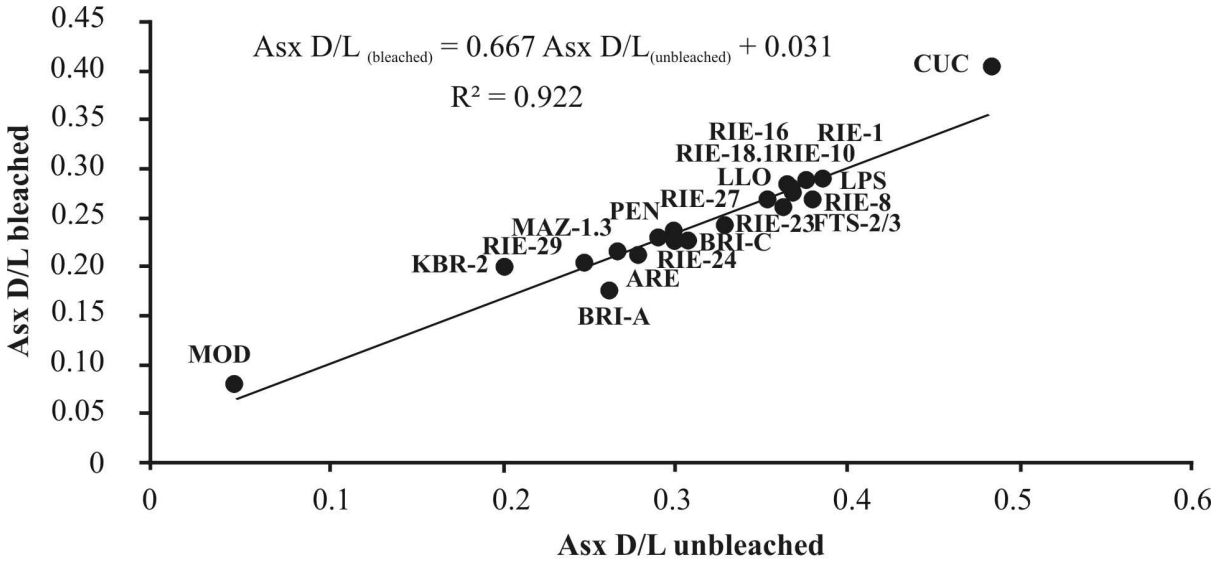
Asx D/L (bleached) = 0.667 Asx D/L(unbleached) + 0.031
R² = 0.922
Asx D/L bleached
Asx D/L unbleached
0.45
0.40
0.35
0.30
0.25
0.20
0.15
0.10
0.05
0
0
0.1
0.2
0.3
0.4
0.5
0.6
CUC
RIE-16
RIE-1
RIE-18.1
RIE-10
LLO
LPS
RIE-27
RIE-8
PEN
RIE-23
FTS-2/3
MAZ-1.3
BRI-C
RIE-29
RIE-24
KBR-2
ARE
BRI-A
MOD

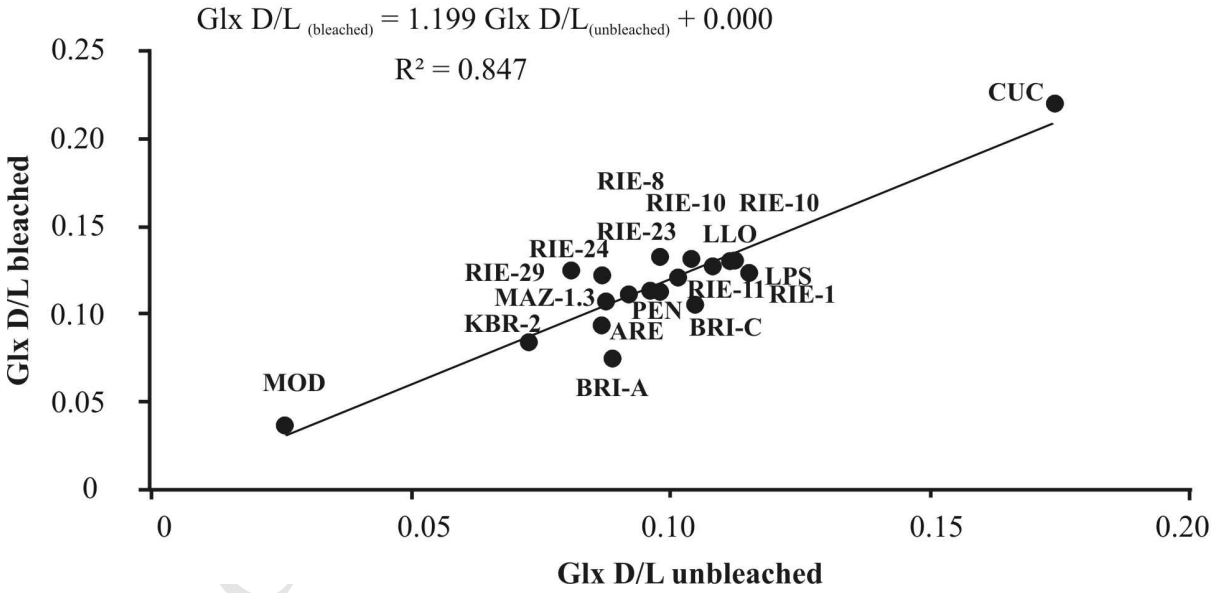
Glx D/L (bleached) = 1.199 Glx D/L(unbleached) + 0.000
R² = 0.847
Glx D/L bleached
Glx D/L unbleached
0.25
0.20
0.15
0.10
0.05
0
0
0.05
0.10
0.15
0.20
CUC
RIE-8
RIE-10
RIE-10
RIE-23
LLO
RIE-24
RIE-29
LPS
RIE-11
RIE-1
MAZ-1.3
PEN
KBR-2
ARE
BRI-C
BRI-A
MOD

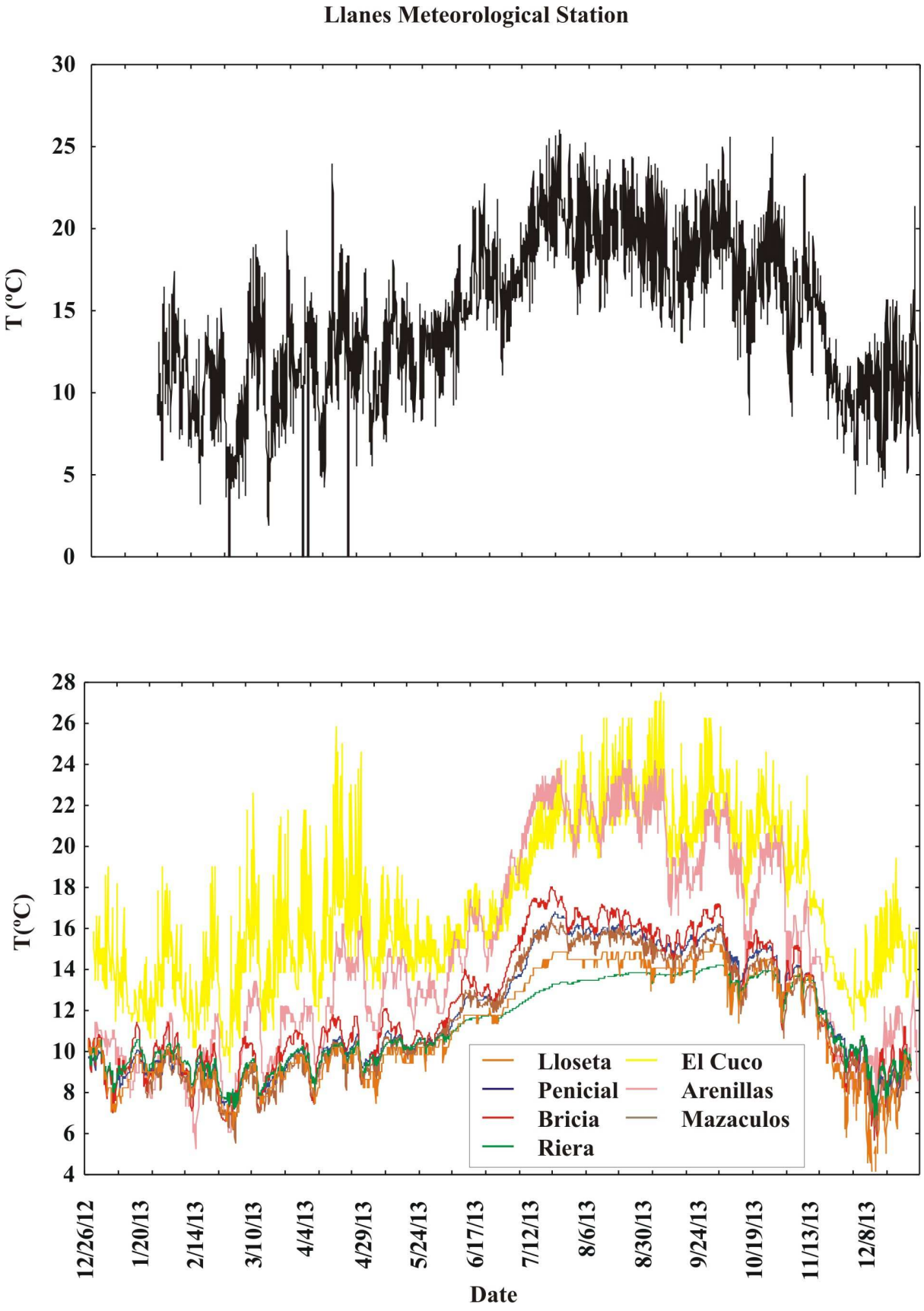
Llanes Meteorological Station
T (ºC)
30
25
20
15
10
5
0
T(ºC)
28
26
24
22
20
18
16
14
12
10
8
6
4
Lloseta
Penicial
Bricia
Riera
El Cuco
Arenillas
Mazaculos
12/26/12
1/20/13
2/14/13
3/10/13
4/4/13
4/29/13
5/24/13
6/17/13
7/12/13
8/6/13
8/30/13
9/24/13
10/19/13
11/13/13
12/8/13
Date

The calcitic apex and rim of *P. vulgata* shells are probably made of similar proteins

The aragonitic intermediate area has a different amino acid composition

The main protein leaching in the inter-crystalline fraction occurs in the first 6 ka

Asp content remained constant up to 34 ka in inter- and intra-crystalline fractions

The percentage of aspartic acid increased with age (over ca. 34 ka)

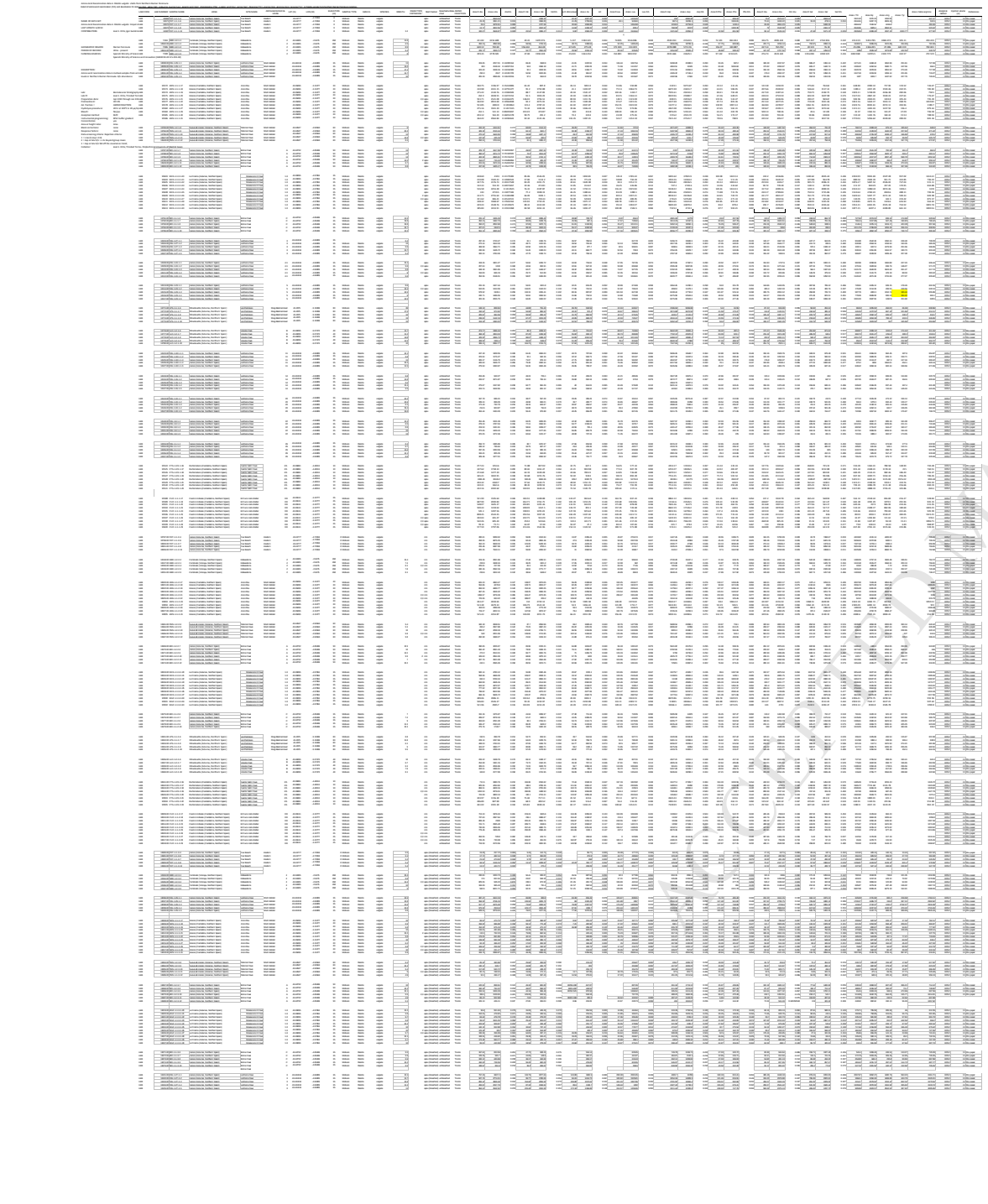

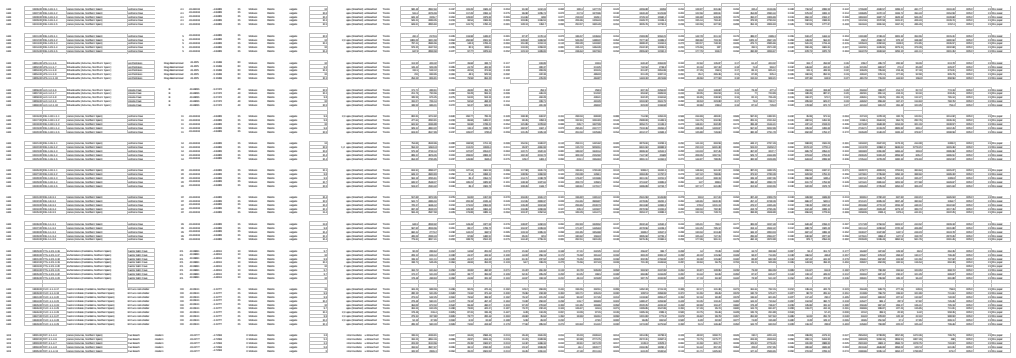

Table 1-Supplementary Data. Radiocarbon ages (yr BP) of the archaeological levels and calibrated ages (cal yr) converted using the Radiocarbon Calibration Program 7.0 (CALIB 7.0) (Stuiver et al., 2014) with the calibration dataset IntCal13 (Reimer et al., 2013).

Locality	Radiocarbon age (yr BP)	Age (cal yr)
KBR-2	5,200±110 yr BP (UBAR-472) [1]	5,975±160
ARE	5,580±80 yr BP (GrN-19596) [2]	6,385±70
BRI-A	6,800±165 yr BP (GaK 2908) [3,4]	7,680±150
MAZ II-1.3	7,700±30 yr BP (UGAM-9081)	8,490±40
RIE-29	6,500±200 yr BP (GaK-3046) [5]	7,375±185
RIE-27	10,630±120 yr BP (BM-1494) [6]	12,510±195
	10,760±400 yr BP (GaK-6985) [6]	17,960±490
RIE-24	10,890±430 yr BP (GaK-6982) [6]	12,660±545
RIE-23	10,340±560 yr BP (Ly-1646) [6]	11,945±730
RIE-18.1	15,230±500 yr BP (Q-2116) [6]	18,430±530
	15,520±350 yr BP (Q-2110) [6]	18,690±490
	16,420±430 yr BP (GaK-6448) [6]	19,680±555
RIE-16	18,200±610 yr BP (GaK-6983) [6]	21,750±770
RIE-10	19,820±390 yr BP (GaK-6447) [6]	23,690±565
RIE-8	20,690±810 yr BP (GaK-6981) [6]	24,810±1055
	15,860±330 yr BP (GaK-6450)	19090±350
RIE-1	19,620±390 yr BP (UCR-1270A)	23485±550
	20,360±450 yr BP (Ly-1783)	24285±565
	20,860±410 yr BP (BM-1739) [6]	24,285±525
PEN	8650±185 yr BP (GaK 2906) [3]	9,760±250
LLO	15,200±140 yr BP (GaK 2549) [3]	18,340±280
FTS-2/3	22,340±510/-410 yr BP (GrN-18574)	26850±775
	22,580±100 yr BP (GX-27756) [7]	27315±385
CUC	30020+160-150 yr BP (GrA 32436) [8]	34,290±160

1.-Zapata Peña et al. (1997) ; 2.-Bohígas and Muñoz (2002) ; 3.-Clark (1976); 4.-Jordá (1957, 1958); 5.-González Morales (1982); 6.- Straus et al., 1978; Straus and Clark, 1986; 7.-Moure and González Morales, 1992; 8.-Muñoz Fernández et al. (2007).

Table 2-Supplementary information. Mean Asx and Glx D/L values in unbleached and bleached samples taken from the apex and rim areas of modern and archaeological *P. vulgata* shells.

Period	Localities	N	Asx D/L Apex	Asx D/L Rim	Asx D/L Apex Bleached	Glx D/L Apex	Glx D/L Rim	Glx D/L Apex Bleached
	Modern	5	0.047±0.006	0.048±0.001	0.079±0.008	0.026±0.004	0.027±0.001	0.036±0.006
N	KBR2	4	0.203±0.008	0.224±0.033	0.199±0.007	0.073±0.013	0.068±0.004	0.084±0.008
M	RIE-29	5	0.248±0.009	-	0.202±0.011	0.081±0.005	-	0.118±0.011
	BRI-A	5	0.264±0.008	0.286±0.015	0.191±0.030	0.089±0.004	0.086±0.008	0.094±0.034
	MAZ II-1.3	9	0.267±0.010	0.256±0.013	0.213±0.018	0.088±0.015	0.072±0.005	0.107±0.021
	ARE	7	0.279±0.020	0.290±0.013	0.212±0.037	0.087±0.010	0.077±0.003	0.093±0.026
	PEN	4	0.292±0.018	0.309±0.026	0.229±0.001	0.098±0.003	0.103±0.030	0.112±0.009
UM	BRI-C	5	0.308±0.023	0.313±0.023	0.225±0.008	0.105±0.008	0.089±0.010	0.105±0.012
	RIE-27upp.	5	0.300±0.018	-	0.223±0.015	0.092±0.004	-	0.111±0.005
	RIE-24	3	0.302±0.020	-	0.227±0.015	0.087±0.001	-	0.121±0.010
	RIE-23	4	0.303±0.004	-	0.242±0.022	0.093±0.007	-	0.138±0.015
LM	LLO	5	0.363±0.018	0.343±0.017	0.260±0.010	0.104±0.006	0.096±0.005	0.131±0.018
	LPS	5	0.387±0.013	0.381±0.012	0.289±0.024	0.115±0.013	0.111±0.012	0.123±0.024
	RIE 18.1	5	0.356±0.018	-	0.267±0.006	0.108±0.016	-	0.126±0.010
S	RIE-16	5	0.369±0.006	-	0.275±0.016	0.111±0.007	-	0.130±0.022
	RIE-10	5	0.378±0.010	-	0.287±0.017	0.112±0.008	-	0.130±0.011
	RIE-8	5	0.379±0.013	-	0.267±0.008	0.101±0.006	-	0.120±0.033
	RIE-1	5	0.370±0.013		0.276±0.025	0.097±0.003	-	0.113±0.008
G	FTS-2/3	7	0.367±0.014	0.374±0.018	0.280±0.010	0.098±0.005	0.119±0.024	0.132±0.028
A	CUC	7	0.484±0.012	0.483±0.027	0.403±0.029	0.174±0.008	0.168±0.016	0.220±0.013

N:Neotlithic; M: Mesolithic (Asturian); UM: Upper Magdalenian; LM: Lower Magdalenian; S: Solutrean; G: Gravettian; A: Aurignacian.

Table 3-Supplementary information. Mean of total amino acid concentrations (pmol/mg) in unbleached and bleached samples taken from the apex and rim areas of modern and archaeological *P. vulgata* shells.

Localities	N	[AA] Apex	[AA] Rim	[AA] Apex Bleached
Modern	5	25477 ± 6340	42771 ± 12320	4095 ± 2510
KBR-2	4	26846 ± 11925	30420 ± 6352	2963±671
RIE-29	5	18107 ± 2216	-	3280 ± 281
ARE	7	18274 ± 5638	24497 ± 2274	4546 ± 4090
BRI-A	5	14554 ± 3733	19396 ± 1795	4922 ± 1522
MAZ II-1.3	9	15934 ± 6426	23906 ± 2997	3399 ± 1402
PEN	5	14816 ± 2132	21363 ± 3356	3100 ± 645
BRI-C	5	14186 ± 4880	15238 ± 2901	4025 ± 1117
RIE-27upper	5	16925 ± 2768	-	3887 ± 674
RIE-24	3	15388 ± 4993	-	3668 ± 617
RIE-23	4	17476 ± 4197	-	3126 ± 368
LLO	5	13349 ± 1073	16170 ± 3123	3631 ± 649
LPS	5	9624 ± 1766	13470 ± 3095	3667 ± 520
RIE-18.1	5	14428 ± 2618	-	3944 ± 1567
RIE-16	5	12288 ± 921	-	4084 ± 1093
RIE-10	5	10066 ± 2071	-	3277 ± 444
RIE-8	5	12759 ± 1669	-	3876 ± 1318
RIE-1	5	12322 ± 4282		4021 ± 780
FTS-2/3	7	15359 ± 3457	15217 ± 7957	3505 ± 455
CUC	7	13437 ± 2451	14540 ± 1558	4117 ± 557

Table 4-Supplementary information. Mean Asx and Glx concentrations (pmol/mg) in unbleached and bleached samples taken from the apex and rim areas of modern and archaeological *P. vulgata* shells.

Localities	N	[Asx] Apex	[Asx] Rim	[Asx] Apex bleached	[Glx] Apex	[Glx] Rim	[Glx] Apex bleached
Modern	5	10616 ± 3165	18154 ± 3489	827 ± 83	1788 ± 347	3361 ± 928	475 ± 434
KBR-2	4	12150±4110	16424±2760	961±544	1903±964	2326±391	351±110
RIE-29	5	10181 ± 1294	-	1237 ± 167	1021 ± 83	-	321 ± 47
ARE	7	10755 ± 3590	14074 ± 1454	1150 ± 518	1032 ± 250	1421 ± 116	588 ± 617
BRI-A	5	8163 ± 2680	13155 ± 1102	1231 ± 289	963 ± 215	1459 ± 201	674 ± 270
MAZ II-1.3	9	8838 ± 4091	13413 ± 1631	947 ± 204	935 ± 295	1379 ± 197	419 ± 245
PEN	4	8709 ± 1315	12380 ± 1657	1091 ± 329	884 ± 215	1347 ± 417	257 ± 60
BRI-C	4	8460 ± 2771	11480 ± 2323	1320 ± 489	812 ± 289	1061 ± 195	371 ± 75
RIE-27	5	10274 ± 1844	-	1672 ± 314	928 ± 144	-	320 ± 41
RIE-24	3	12172 ± 1256	-	1567 ± 443	895 ± 288	-	321 ± 22
RIE-23	4	10797 ± 3052	-	1276 ± 222	977 ± 206	-	298 ± 25
LLO	5	8449 ± 584	9813 ± 1566	1490 ± 335	719 ± 89	935 ± 218	292 ± 44
LPS	5	6045 ± 1347	8493 ± 1988	1631 ± 296	568 ± 57	793 ± 187	306 ± 49
FTS-2/3	7	9848 ± 2249	8860 ± 5040	1384 ± 176	862 ± 205	946 ± 420	336 ± 77
RIE-18.1	5	9363 ± 1682	-	1863 ± 890	767 ± 171	-	329 ± 116
RIE-16	5	7867 ± 1336	-	1921 ± 644	624 ± 71	-	338 ± 62
RIE-10	5	6531 ± 1453	-	1501 ± 217	533 ± 94	-	280 ± 38
RIE-8	5	7846 ± 701	-	1478 ± 331	724 ± 140	-	381 ± 165
RIE-1	5	8939 ± 2552	-	1824 ± 441	658 ± 185	-	333 ± 52
CUC	7	8873 ± 1669	9342 ± 1161	2036 ± 364	782 ± 137	896 ± 84	340 ± 35

Table 5-Supplementary information. Percentage of each amino acid concentration in the apex, rim and intermediate areas of modern *P. vulgata* shells.

Area	Asx	Glx	Ser	Ala	Val	Phe	Ile	Leu	Thr	Gly	Arg
Apex	41.1±3.6	7.2±1.0	9.4±0.3	7.2±1.0	3.8±0.5	2.4±0.7	3.3±0.6	2.8±1.2	5.7±0.4	11.5±0.8	5.6±0.3
Rim	42.1±2.5	7.6±0.4	9.6±0.5	7.2±0.5	4.0±0.2	2.0±0.3	3.2±0.1	3.0±0.7	5.7±0.2	10.2±0.8	5.7±0.2
Intermediate	39.6±2.4	8.0±0.4	8.9±1.0	8.1±0.2	4.9±0.3	2.1±0.2	3.6±0.2	4.3±0.4	5.7±0.4	8.9±0.6	6.0±0.3

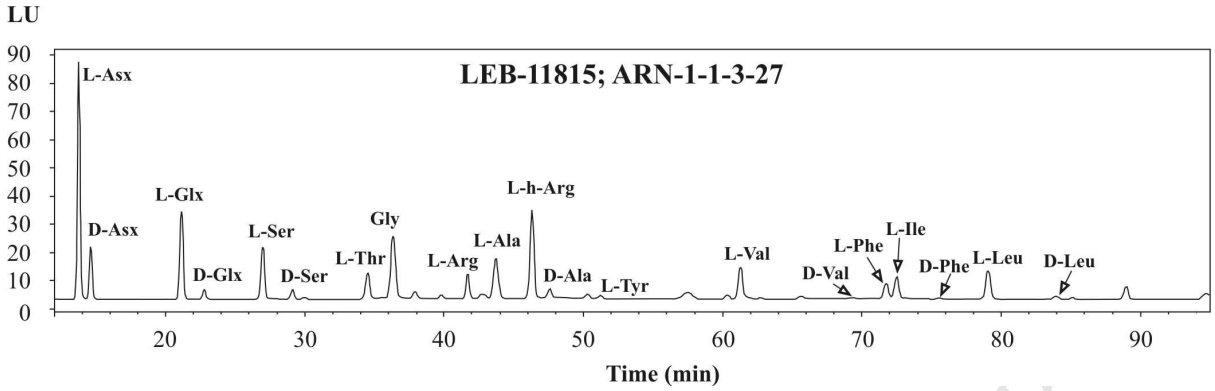

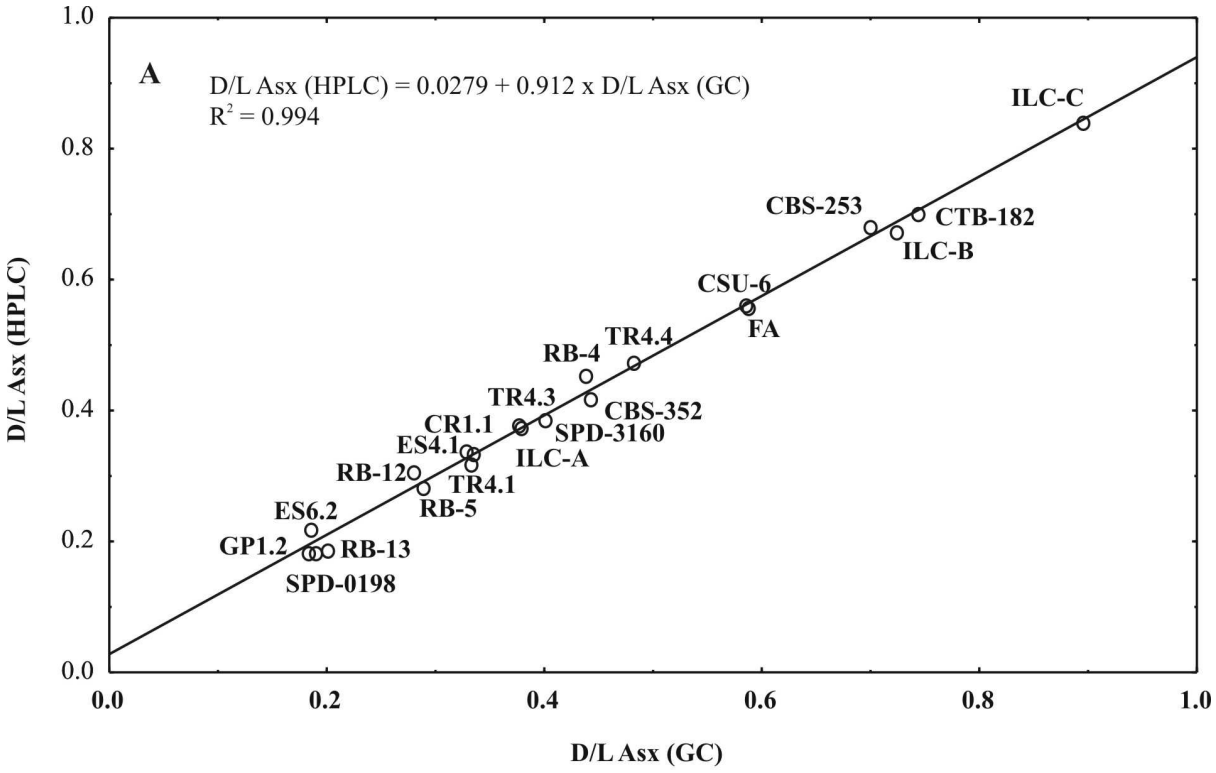
A
D/L Asx (HPLC) = 0.0279 + 0.912 x D/L Asx (GC)
R² = 0.994
D/L Asx (HPLC)
D/L Asx (GC)
0.0
0.2
0.4
0.6
0.8
1.0
ILC-C
CBS-253
CTB-182
ILC-B
CSU-6
FA
TR4.4
RB-4
TR4.3
CBS-352
CR1.1
SPD-3160
ES4.1
ILC-A
RB-12
TR4.1
RB-5
ES6.2
GP1.2
RB-13
SPD-0198

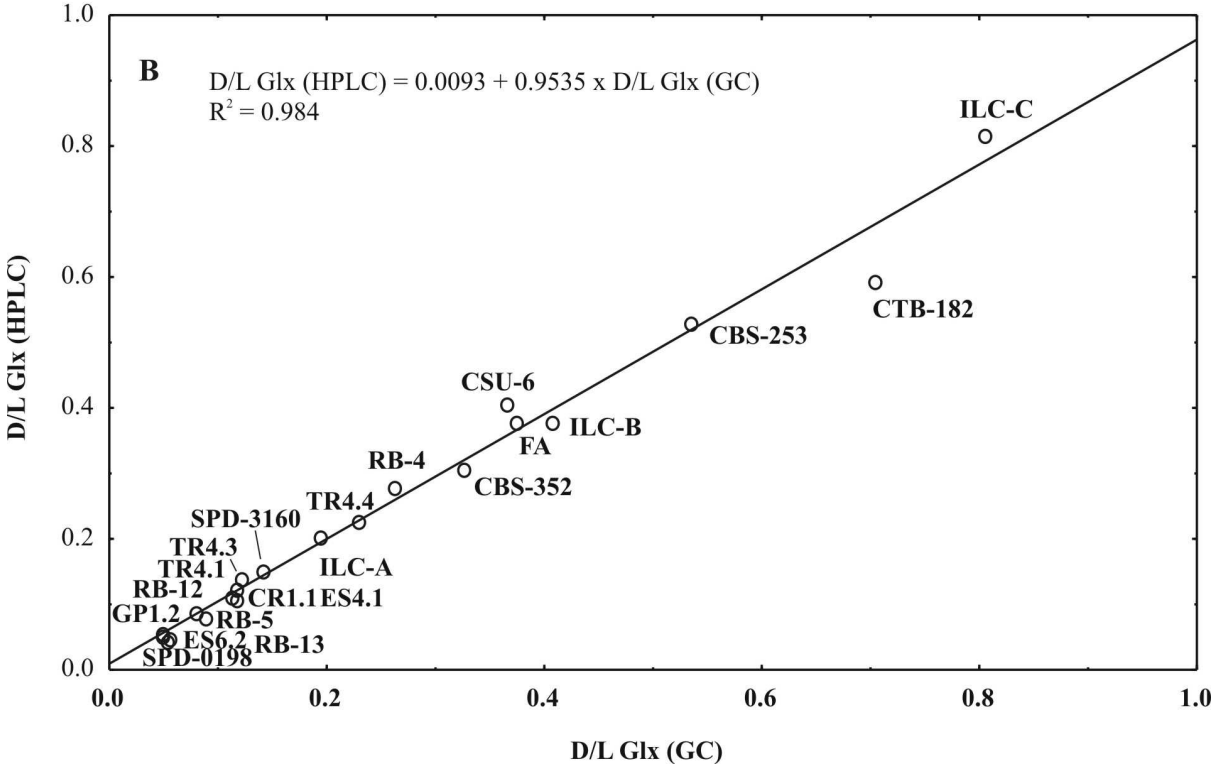
B
D/L Glx (HPLC) = 0.0093 + 0.9535 x D/L Glx (GC)
R² = 0.984
D/L Glx (HPLC)
D/L Glx (GC)
0.0
0.2
0.4
0.6
0.8
1.0
ILC-C
CTB-182
CBS-253
CSU-6
ILC-B
FA
RB-4
CBS-352
TR4.4
SPD-3160
TR4.3
ILC-A
TR4.1
RB-12
CR1.1
ES4.1
GP1.2
RB-5
ES6.2
RB-13
SPD-0198